Knut Vilhelm Høyland

Measurements and simulations of consolidation in first-year sea ice ridges, and some aspects of mechanical behaviour

NTNU Trondheim
Norges teknisk-naturvitenskapelige universitet

Doktor ingeniøravhandling 2000:94
Konstruksjonsteknikk

Measurements and simulations of the consolidation in first-year sea ice ridges, and some aspects of mechanical behaviour.

Knut V. Høyland
Department of Structural Engineering
The Norwegian University of Science and Technology

September 2000

Abstract

The thesis deals with the consolidation process in floating first-year sea ice ridges, but some aspects of mechanical behaviour related to ridges and ridging are also discussed. Numerical simulations, field measurements and laboratory work have been performed. Four different in-situ ridges and the surrounding level ice conditions as well as three laboratory made ridges have been studied. The two first ridges were examined the winter of 1998 at Spitsbergen. One was situated in front of the Tuna glacier in the Tempel fjord, and the other off Svartodden in the western part of the Van Mijen fjord. The following winter two more ridges were studied; one off Camp Morton in the Van Mijen fjord on Spitsbergen and another outside Marjaniemi scientific station at the island Hailuoto west of Oulu in Finland. The laboratory work was carried out in the Large Ice Tank of the Hamburg Ship Model Basin (HSVA) in Hamburg, Germany the autumn of 1999.

Geometry, morphology and salinity were examined in all four ridges, whereas measurements of spatial and temporal temperature development were done in three of the ridges (Svartodden, Camp Morton and Marjaniemi). The density and the crystal structure were studied in the two 1999 ridges, and small-scale uniaxial compression tests of the consolidated layer were done only on ice from the Marjaniemi ridge. In the Tempel fjord the formation of the ridge-field and the creep buckling of the level ice prior to ridging were studied. The laboratory work included examinations of salinity, density and temperature development, small-scale mechanical testing and plug tests. In the plug test the consolidated layer was cut and the rubble loaded vertically until failure.

The ratio of the average thickness of the consolidated layer divided by the thickness of the level ice, R_{avg}, has been estimated by the use of recorded temperatures and by drilling results. The temperatures gave R_{avg} values ranging from 1.39 to 1.61, whereas the drillings gave 1.68 – 1.85. Thus, the method of investigation affected the results. The small-scale compression tests (without temperature corrections) corresponded better with the temperature-derived thickness of the consolidated layer than with the drilling results. The drillings probably included the partly consolidated layer. The average growth of the consolidated layer ranged from 0.45 to 1.02 cm/day, and did not depend on the applied method. The consistency of the unconsolidated part of the keel differed between the ridges examined in the Van Mijen fjord and the one off Marjaniemi. This was due to differences in salinity, surrounding currents and the shapes of the keels.

The movement of the Tuna glacier probably provoked the formation of the ridge-field in the Tempel fjord. The speed of the glacier was measured to 0.23 m/day, and up to four parallel ridges developed during the

spring. Ice block thicknesses of 0.2 m were observed in a ridge that was made from one metre thick level ice.

In the laboratory ridges, R_{avg} was higher than what was measured in-situ; this is probably due to high initial growth in the laboratory. Different 'oceanographical' conditions and effects of scaling may explain this. The strength of individual ice pieces from the ridge was higher than that of level ice. This was because the level ice was warmer than the ridge. It seems to be difficult to achieve correctly scaled temperature fields in the ice tank.

A numerical finite element model to study the heat transfer processes in first-year sea ice ridges has been developed. The program ABAQUS with user-defined subroutines to calculate the thermal load has been applied. The four surface heat fluxes: the sensible flux (q_{sens}), the sublimation flux (q_{subl}), the long-wave flux (q_{long}) and the short-wave flux (q_{sol}) constituted the thermal load. They were calculated by the use of the surface temperature of the ridge, the meteorological data and the spatial and temporal location. The porosity of the ridge was treated in two different ways; 1) creating a composite material consisting of sea ice and water with ordinary sea ice/water thermal properties and 2) defining a homogeneous equivalent material. A model with purely conductive internal heat transfer simulates the measured growth of the consolidated layer and the level ice well. But modifications of the model are necessary to handle the initial phase of ridge consolidation that seems to be dominated by convection. One-dimensional simulations have been used to estimate the theoretical limit of the ratio of the thickness of the consolidated layer to the thickness of the level ice. Limit values as functions of the porosity have been found. The question of whether this limit is a maximum value or not, is determined by the initial phase. If the consolidated layer during the initial phase does not exceed this limit value it becomes a maximum, and vice versa.

Acknowledgement

The writing of a doctoral thesis is often described as a lonely struggle. Somehow I have not really felt it like that. Thanks to my supervisor Professor Sveinung Løset I have had good co-operation with and help from several people. The help has ranged from practical help in the field to computer trouble shooting. I would very much like to thank the following people who have made my strive easier and less lonely:

The siv.ings Arne Langeland, Guro Kjestveit and Morten Khyring, many of the students at UNIS during the winters 1998 and 1999 as well as the staff at UNIS. They all contributed in making the field work possible.

Jaakko Heinonen and Professor Mauri Määttänen from the Helsinki University of Technology (HUT) who let us participate in their fieldwork the winter of 1999 in the Gulf of Bothnia. We have also had many fruitful discussions, and finally they have taken care of me during my visits to Ottaniemi. The technical crew from HUT did a lot of excellent work during the fieldwork, and their assistance is also appreciated.

The Norwegian Research Council has paid my scholarship for three years.

The LOLEIF project (the framework of the EU-sponsored Marine Science and Technology (MAST-III) programmed under contract no.MAS3-CT97-0078) paid most of the extra expenses. I have also had the opportunity to present preliminary versions of the different parts of my work to the LOLEIF group. This has been very inspiring and useful, and I would especially like to thank Jeff Weaver from Exxon.

The INTAS project (97-16665) has also been a source of inspiration and help and I would like to thank the initiator of this project Tuomo Kärnä.

I have been so lucky to be able to participate in experiments in The Hamburg Ship Model Basin (HSVA) in Hamburg, Germany. HSVA has also bee the leader of the LOLEIF project and Dr. Joachim Schwarz, Karl-Ulrich Evers, Jens-Holger Hellman and the technical crew have definitely contributed in a positive way to my work.

During my two months stay in St.Petersburg at the St. Petersburg State Technical University (SPTU) Professor Karl Shkhinek took good care of me and let me sit in the warm room. He has also spent his time on several occasions while trying to elucidate me.

My colleague from NTNU Arnor Jensen is the principle author of one of the papers. We have worked together in HSVA and have had many interesting discussions. He has also read through several of the papers and must be said to be responsible for several improvements.

Martin Henriksen and Dag Anders Moldestad have tried to transfer basic knowledge about the digital world into my head. If their effort have been in vain it is my fault and not theirs.

And finally I would like to express my gratitude to my supervisor Professor Sveinung Løset for inspiration, help, fruitful discussions, never-ending enthusiasm and for introducing me to the international ice community. This has all been important for me in my work towards this dissertation.

Ice is supposed to be water below the freezing point
If one examines an ice crystal more closely,
the explanation seems inadequate.

Ivan Malinowskij, 1983

Table of contents

Chapter 1

Introduction

1.1 Motivation

Sea ice ridges are formed by compression or shear in the ice cover, and has been a well known curse for human beings in the Arctic as long as people have been trying to move around up there. On the boat back from Spitsbergen after the famous 86°14' expedition the Norwegian scientist and adventurer Fridtjof Nansen wrote in his diary that he would never ever go back to the ridges, and he kept his vow. His colleague Hjalmar Johannesen was already longing back into the ice...

Why should one then spend three years (and three months) to study these ice features that Nansen had taken such a distinct dislike of? From a personal point of view it has given me the opportunity to travel and experience fantastic nature, interesting cities and get to know many nice people. Strangely enough this does not seem to have been the motivation of the Norwegian Research Council who paid my scholarship, or the EU funded LOLEIF (Validation of Low Level Ice Forces) project that paid most of the extra expenses. They seem to have taken more interest in trying to solve practical problems concerning human activity in marine Arctic and sub-Arctic areas. In many of these waters (e.g. the Barents Sea, the Pechora Sea and the Gulf of Bothnia) first-year ice prevails and ice ridges may represent the design ice feature for man-made structures such as platforms, ships, pipelines, bridges, docks and perhaps even wind-mills. The forces involved in an ice ridge – structure interaction are not well known. The deformation modes of the ridges are neither well known. The basic reason for this uncertainty is the lack of knowledge about the internal structure of a first-year sea ice ridge and its seasonal development. The thickness and strength of the level ice and the meteorological conditions are both better-known and easier to measure, thus an important task is to relate the internal structure of an ice ridge to this easier accessible information.

But there are also other reasons for studying ridges than the purely engineering ones. From a geophysical point of view ridges are of interest in relation to e.g. large-scale constitutive models of ice. Energy is consumed in the ridging process i.e. it acts as a sink. Depending on their degree of consolidation, ridges represent zones of strength or weakness in the ice cover.

Thirdly I would like to point at another motivation for doing research, namely the profound human curiosity, the desire to make sense out of things, to establish an explanation with which we are comfortable. This urge lead human beings into theoretical and practical investigations with no particular motivation in mind but the question: Why is so that...?

1.2 Object, scope and organisation of the thesis

The intent of the thesis has been to gain increased knowledge about the internal structure of first-year sea ice ridges and its seasonal development, and further to compare with the level ice conditions. A combination of in-situ fieldwork, laboratory experiments and theoretical numerical analysis has been performed. The main objectives were:

- In-situ field measurements:

  To examine the geometry, morphology, spatial and temporal temperature development, physical and mechanical properties and ice texture in first-year sea ice ridges, as well as to measure the surrounding level ice conditions and the meteorological conditions.

- Laboratory experiments:

  To investigate the corresponding properties of laboratory made ridges in order to move towards an accepted method of scaling thermal and mechanical properties of ridges.

- Numerical work:
  To develop a numerical code that simulates the measured temperature development in the ridges and the level ice as a function of the meteorological conditions and the physical properties.

The content of the thesis is six individual papers submitted to or accepted in international journals or conference proceedings. Chapter 2 to 4 deals with the thermodynamics of ridges: theoretical concepts, measurements and simulations. In the three subsequent papers problems related to mechanical behaviour, physical properties and scaling of ridges are discussed.

Chapter 2 discusses theoretical concepts and definitions related to the consolidation of ridges. It also presents the main results of the field investigations.

Chapter 3 describes and discusses the measurements of temperature distribution, consolidation and morphology of the first-year ice ridge that was surveyed in the Van Mijen fjord in the winter of 1998.

Chapter 4 deals with the numerical work. It describes the development of – and the results from the finite element model that has been used to simulate the measured temperature development in the ridges and in the level ice.

Chapter 5 presents and discusses the measurements of the physical and mechanical properties of the consolidated layer of the ridge off Marjanimei weather station in Finland the winter of 1999. The thermal and the mechanical definitions of the thickness of the consolidated layer are also discussed.

Chapter 6 describes the monitoring and observation of the formation of a first-year ridge-field in front of the Tuna glacier in the Tempel fjord on Spitsbergen during the spring of 1998. The deformation mechanisms in the ridging process including creep buckling, fracturing and splitting are discussed.

Chapter 7 covers the laboratory work carried out in the Large Ice Tank of the Hamburg Ship Model Basin (HSVA) in Hamburg, Germany the autumn of 1999. It describes the measurements done on the three ridges and discusses the scaling of thermal and mechanical properties of ridges.

Chapter 8 presents the main conclusion from the six papers and suggests possible further work.

1.3 Readership

I hope that this thesis can contribute to increase the understanding of the nature of the consolidation process in first-year sea ice ridges, and that it can be a part of the background when design criteria for Arctic structures are to be made. I also hope it communicates the importance of doing experimental, numerical and theoretical investigations hand-in-hand. The primary readership targeted by this thesis is:

- Engineers and scientists working with sea-ice related problems, especially those that work with ice-structure interaction or air-sea-ice interaction.

- Students and teachers dealing with problems related to sea ice in any form. Parts of the thesis may serve as an introduction to the thermodynamics of ridges.

Chapter 2

The consolidation of first-year sea ice ridges

Submitted to the Journal of Geophysical Research

Notation

Symbols:

η	macro porosity
η_t	total porosity
q	heat flux per unit surface area
T	temperature
h	height / thickness
w	width
FDD	cumulative freezing degree days
t	time
R	the thickness of the consolidated layer divided by the thickness of the level ice
k	thermal conductivity
l	latent heat of phase change
ρ	density
σ	stress
ω	coefficient in Stefan's law
b	coefficient to account for the difference in insulation of the level ice and a ridge

Indices:

sur	surface
c	consolidated layer
re	internal redistribution
$ocean$	oceanic
$sens$	sensible or convective
$subl$	sublimation
$long$	long-wave
sol	solar
f	freezing point
s	sail
k	keel
b	block
air	air
avg	average

max	maximum
i	sea ice
pi	pure ice
r	rubble
T	temperature
D	drillings

The consolidation of first-year sea ice ridges

Knut V. Høyland

Norwegian University of Science and Technology (NTNU)

Trondheim, Norway

The University Courses on Svalbard (UNIS)

Longyearbyen, Norway

knut.hoyland@bygg.ntnu.no

Abstract

Measurements of spatial and temporal temperature development, geometry, morphology and physical properties in three first-year seas ice ridges at Spitsbergen and the Gulf of Bothnia have been done. The corresponding thickness and physical properties of the surrounding level ice were also measured. The thickness of the consolidated layer was examined by the use of drilling and by the use of the temperature measurements; the temperatures gave a ratio of the thickness of the consolidated layer to the level ice thickness from 1.39 to 1.61, the drillings gave 1.68 - 1.85. The measured consolidated layer turned out to be 28 % thicker when using drillings than when using temperatures. Thus, the result depended on the method of investigation; the drillings included a partly consolidated layer. However, the measured growth of the consolidated layer did not depend on the method of investigation. The scatter of the physical properties in the consolidated layer was higher than that of the level ice. The consistency of the unconsolidated rubble was clearly different at the two sites. It was soft and slushy at Spitsbergen, and harder in the Gulf of Bothnia. Three possible reasons are discussed: surrounding currents, different keel-shapes and the difference in salinity.

1. Introduction

Sea ice ridges are formed by compression or shear in the ice cover. Environmental forces such as winds and currents can create substantial stresses in an ice cover. If these stresses exceed the strength of the ice at some point in the floe, a deformation process starts. Sea ice cover deformation is characterised by localised failure. The deformation often starts in a refrozen lead in which the ice is weaker than in the surrounding ice. Nevertheless, it may also occur in ice covers without refrozen leads. Ridging and rafting are the two basic deformation modes when ice sheets are compressed or sheared. Rafting describes the situation where two ice sheets that are driven against each other override without any further deformation. The process continues until the friction forces exceed the driving forces. In ridging the ice cover is broken, and a pile of broken ice, water, snow and air is created. The volume over the waterline is called the sail, and the pores in this part are filled with air or snow. Most of the volume is below the waterline, the keel. The phenomenon of ridging involves many problems of interest to engineers and researchers, spanning from small-scale mechanical properties and fracturing of ice blocks to large scale constitutive modelling of sea ice. Aspects such as the kinematics and the kinetics, the onset and duration of a ridging process and the energy consumed have been studied by several researchers. Pioneer work was done by Parmerter and Coon [1972 and 1973]. Fig. 1 shows a ridge in the Van Mijen fjord the winter of 1997.

<Fig. 1>

Ridges often exist in combination with rafted ice and the combination can then be defined as a ridge-field. Ridges and ridge-fields are often found in the shear zone between the landfast ice and the drift ice. A high ridge density may also be found in straits and sounds with strong currents. Rubble fields also form in front of obstacles such as large structures due to ice drift or thermal activity. Ice ridges are in general long and curvilinear; i.e. they are three-dimensional features. Fig. 2 shows a ridge in front of the Tuna glacier in the Tempel fjord on Spitsbergen in March 1998. Ridges that survive the summer and live into a new winter are called multi-year ridges; their geometry and morphology differ some from first-year ridges. Some researchers also distinguish between second- and multi-year ridges. The characterisation of ice ridges is often done by studying one or several cross sections. Geometrical ratios such as keel depth to sail height, keel depth to keel width and keel area to sail area are often given [see Timco and Burden 1997 for a summary of ridge geometries]. Typical keel depth/sail height ratios are 4.5/3.3 for first-year/multi-year ridges. The porosity (η) is another important characteristic, it is usually defined as the ratio of the volume of any non-sea ice material to the total volume. As the season proceeds the porosity decreases, because the water in the pores freeze up. This creates a frozen zone that grows downwards in the ridge; i.e. the ridge is consolidating. The consolidation process in first-year ridges is the main focus of this paper.

<Fig. 2>

Ridges are important ice features and may represent the design load for ships, coastal and offshore structures in many arctic and sub-arctic marine areas. However, it is not clear what load a first-year ridge can exert on a given structure or how the ridge deforms. It depends on the age and composition of the ridge as well as the structure. Different ridge failure modes observed at the Molikpaq platform is presented by Timco et al. [1999]. For a large number of the ridges, the first failure occurred in the level ice behind the ridge. The ridge itself failed in different modes: shear, bending or spine failure. They report that the measured loads were lower than those given by different load algorithms. The loads are usually calculated by assuming that the load contributions from the sail, the consolidated layer and from the keel can be found independently and then added together [see e.g. Krankkala and Määttänen 1984]. Increased knowledge about the internal structure of first-year ridges is necessary to improve these load estimates. The worst case scenario for the consolidated layer is crushing. Thus, its size and crushing strength are of special importance. The rubble is usually assumed to behave as an elastic plastic material with Colomb-Mohr yield criterion until failure, and as a viscous fluid in continuous deformation.

2. Thermodynamics of ridges

2.1 Thermal processes and energy transport

The consolidation of a ridge is a complex process involving both conductive and convective heat transfer. Mechanical erosion may also be important. Four different energy transfer fluxes can be identified:

- heat flux out through the air exposed surface, q_{sur}
- flux up through the consolidated layer, the sail and the snow cover, q_c
- internal redistribution of energy, q_{re}
- heat transfer from the ocean, q_{ocean}

From Fig. 3, we see that different mechanisms are responsible in different parts of a floating ridge. In a grounded ridge, a stamucha, it is also necessary to consider the temperatures in - and the heat flux from the sea bottom. The surface flux, q_{sur}, is a combination of convection, sublimation, long- and short-wave radiation, q_c is basically a conductive term, q_{re} is a mixture of conduction and convection whereas the oceanic flux is a convective term.

<Fig.3>

One may distinguish between two different phases in time: an initial phase and a main phase. The internal redistribution and the flux from the ocean are crucial in the initial phase. Cold ice blocks are submerged into warm water and energy is exchanged. The ice surfaces exposed to the surrounding water gain energy from the ocean, whereas the fluxes through the internal surfaces redistribute the energy internally in the keel. Due to the permeability of the keel, convective heat flux may also be added through the internal surfaces. The temperatures in the keel approach the freezing point of the ridge material (T_f). However, energy is still being transferred between the ice and the water/slush in the pores, but it is now consumed by phase change and is therefore not reflected as a temperature change. The duration of the initial phase is a function of the oceanographical conditions, the permeability of the keel, the initial temperature and the thickness of the ice blocks. At the end of the initial phase, the keel can be divided into two parts: a cold upper frozen part (the consolidated zone) and a lower unconsolidated part in which the temperatures are close to T_f. In the main phase, the energy transport up through the consolidated layer and out through the air-exposed surface is the dominating process. This phase continues throughout the cold season and is governed by the meteorological conditions. The surface flux q_{sur} can be divided into the following terms:

$$q_{sur} = q_{sens} + q_{subl} + q_{long} + q_{sol} \qquad (1)$$

where q_{sens} is the sensible or convective heat flux, q_{subl} the sublimation heat flux, q_{long} the long- wave heat radiation and q_{sol} the short-wave or solar radiation.

The short wave radiation (q_{sol}) is a function of latitude, day, time and cloudiness [Ashton, 1986], whereas the three other terms (q_{sens}, q_{subl} and q_{long}) can be estimated from the air temperature, the surface temperature, the wind speed, the relative humidity and the cloudiness [see e.g. Løset, 1992; Maykut, 1986]. The surface temperature is also crucial for the conductive flux up through the consolidated layer, the sail and further up through the snow. The temperature gradient through these layers as well as their size and thermal properties determine q_c. The snow cover has an important insulating effect that has to be taken into account in any model created to estimate this flux. It is a multi-layer complex structure in constant transformation and precise measurements are necessary to characterise it properly [Granberg, 1994]. A non-symmetrical snowdrift around a ridge creates a non-symmetrical consolidated layer [Høyland and Løset, 1999a]. Most of the energy that is transported upward (q_c) and into the cold air originates from latent heat released as the pores freeze up.

Latent heat is released and transported upwards as a pore freezes. It is reasonable to assume that the initial salinity of such a water pocket is that of the surrounding seawater. Measurements of salinity in a partly frozen pore in an ice-tank ridge show higher salinity than the neighbouring ice, but less than the water [Jensen et al., 2000]. Examination of the salinity in neighbouring ridges of different ages shows substantial differences in salinity: 4 - 7 ppt in the old ridge and 9 - 29 ppt in the young ridge [Høyland and Løset, 1999b]. Several measurements of salinity in ridges have revealed little difference between the salinity of level ice and that of the consolidated layer [see e.g. Kankaanpää, 1997; Leppäranta et al., 1995; Frederking and Wright, 1982]. All these results indicate that brine is drained quite efficiently in the consolidated layer. However, it is not clear what the salinity distribution in the unconsolidated rubble looks like.

2.2 The consolidated zone

The formation and growth of the consolidated zone is the most striking seasonal development of the internal structure in a first-year ice ridge. It is however not clear how the consolidated layer should be defined, nor does it seem to exist a standardised method for examining the thickness of this layer. The water line is often used as an upper boundary as the blocks are loosely bound in the sail. The lower boundary is more difficult because there exists a partly consolidated layer beneath the fully refrozen one. This partly consolidated layer is a porous high temperature zone with less mechanical strength than the fully refrozen one, but the strength is probably higher than that of the unconsolidated rubble. The determination of the lower boundary can be done either in a thermal-, or in a mechanical sense. If the thermal one is chosen, then the temperature becomes the prime indicator of consolidation. The temperatures in the consolidated layer are said to be below the freezing point. Measurements can be made by coring or by installing thermistor-strings. The thermal definition has the advantage that it is precise and that it is clearly related to measurements. It is also relatively easy to do continuous measurements. The disadvantage is that it excludes the partly consolidated layer and that it is more time and money consuming than drilling. A mechanical definition will be related to a pronounced drop in some mechanical strength at a certain depth level. The best way to examine this is to take samples from different depths, and do e.g. uniaxial compression tests. This is even more time and money consuming, so mechanical drilling is often used. Now two possible criteria can be used: The consolidated zone can be defined to extend down to the first pore, or the driller can feel the change in resistance as the drillbit enters the unconsolidated part. The major advantage of drilling is that it is quick to perform. It is however less precise as it depends to some extent on the driller. Drilling is also a destructive method so it becomes more difficult to examine the temporal development of the consolidated layer. The thermal definition seems to estimate a thinner consolidated layer than what is found by drilling. This is probably because a thermal definition excludes the partly consolidated zone. There are also other methods such as the Arctic and Antarctic Research Institute's (AARI) hot point needle or some other thermal drilling system. See Mironov et al. [1999] for a discussion of thermal versus mechanical drilling to examine ridges. However, uniaxial compression tests, without temperature corrections, seem to correspond with temperature measurements [Høyland et al., 2000].

The internal structure of a ridge is not directly observable, hence it is of great interest to relate it to more easily observable quantities such as meteorological and oceanographical conditions and level ice thickness. Numerical finite element simulations of conductive heat transfer within the ridge and with the meteorological conditions giving the thermal load (q_{sur}) using ABAQUS has been done. The simulations predict the measured growth of the consolidated layer [Høyland, 2000]. Another easy way to estimate the thickness of the consolidated layer is to compare with the level ice thickness. Adjacent level ice is subjected to the same physical environmental loads as the ridge, but it grows with another speed. A simple analytical model based on Stefan's law is developed by Leppäranta and Hakala [1992], it relates the thickness of the consolidated layer to the porosity of the ridge and the thickness of the level ice. The ratio of the size of the consolidated layer over the level ice thickness has been studied by several researchers [e.g. Kankaanpää, 1997; Leppäranta et al., 1995; Croasdale et al., 1990; Timco and Goodrich 1988; Frederking and Wrigth, 1982], and the reported results are from 1.2 to 1.9. It is however not always clear whether a thermal or a mechanical definition is used. Measurements in three first-year ridges reported in this paper gave a ratio of 1.39 - 1.61 when a thermal definition is used and 1.68 - 1.85 when using the drilling results. However, the growth of the consolidated layer was not dependent on the method of investigations and ranged from 0.45 – 1.02 cm/day.

2.3 The deterioration of the keel

A less dramatic but still important process is the deterioration of the lower part of the keel. Energy is as we have seen redistributed internally (q_{re}), and gained from the ocean (q_{ocean}). Therefore, new ice crystals may be formed in the pores at the same time as the blocks become softer. If there is enough time, the blocks and the pores will approach a slushy consistence. The importance of this process is not yet elucidated, more experiments and theoretical work is necessary. Of importance for the process may be the salinity of the seawater and thereby the porosity of the level ice, the permeability and the shape of the keel, and the surrounding oceanographical conditions. When the ice blocks are submerged water penetrates into the vacated brine channels or any other porosity. This increases the effective area through which energy can be transferred and thereby the speeds of the deterioration process. The speed and temperature of the surrounding currents together with the permeability of the keel give the oceanic flux and this may be of high importance. The surface divided by the volume of the keel is also important as it determines the energy/volume that is added to the keel. The oceanic flux is a difficult problem in oceanography and much is yet to be done. The source of this might be upwelling of deeper water or the incoming of warmer water. Maykut and Perovich [1987] suggest 2 W/m^2 as an annual average for the Arctic basin, and this seems to be an accepted value [Heil et al., 1996]. However, seasonal variations from 0 to 18 W/m^2 have been measured off the coast of East Antarctica [Heil et al., 1996]. Average values for the eastern Weddel Sea range from 2 to 40 W/m^2 [Lytle and Ackley, 1996]. These estimates are done for level ice, but the flux into a ridge keel may be higher due to the permeability and the exposed area/volume of the keel.

2.4 The porosity

Two levels of porosity can be considered: macro porosity η and total porosity η_t. The macro porosity η is the ratio of the volume of any non-sea ice material to the total volume. This is what is usually meant by the porosity of a ridge. This porosity is commonly measured by drilling holes along a cross-section of a ridge and registrating any drop of the drill as a pore. It is easily established early in the season, or as long as the blocks can be distinguished from the pores. Later in the season, it may become more problematic as the consistency of the blocks and the pores approach slush. Most of the reported values are between 30 and 35 % [see e.g. Kankaanpää, 1997; Coon et al., 1995; Leppäranta and Hakkala, 1992 and Veitch et al., 1991a; Frederking and Wrigth 1982]. Theoretical calculations of porosity of a volume consisting of perfect spheres give a porosity between 25 and 40 %, A total porosity can be defined by including the porosity of the level ice from which the ridge is formed. In this case, there are two possibilities. It can be defined as the ratio of the volume of any non-pure ice material (including air pockets) to the total volume, or as the ratio of the volume of liquid (excluding the air) to the total volume. Measurements of this kind of porosity can be done with a thermal drill (e.g. AARI's hot point needle). Beketsky et al. [1997] report an initial hummock porosity of 44 - 47 %, and this may represent the total porosity. Simple theoretical calculations of a total porosity may be done. If one assumes an ice sheet as shown in Fig. 4, and uses the equations of Cox and Weeks [1983], it is reasonable to expect a porosity of the level ice of 10 - 12 %. A ridge with a macro porosity of 35 % made from this level ice would then have a total porosity of 42 - 43 %. Finite element simulations of the heat transfer process in ridges support the idea of a total porosity [Høyland, 2000].

<Fig. 4>

Seasonal development of the porosity η of the unconsolidated parts of the keel has been done, Leppäranta et al. [1995] found no change, whereas Høyland et al., 2000] found indications of a decreasing porosity. The porosity does not seem to be evenly distributed vertically, a mid-keel minimum has been measured [Leppäranta et al., 1995; Lensu, 1993].

The porosity of the consolidated layer is interesting in a mechanical model. Measurements of consolidated zone porosity η done by drilling 2" holes are reported by Høyland and Løset [1999a]. The porosity of the consolidated and the partly consolidated layer of the ridge were found to be 3.4 %, but most of these pores were located in the lower part. Little evidence was found of pores in the colder parts. This may be because there were none, that they were smaller than could be detected with the present equipment (a few centimetres), or that they had frozen. It is obvious that small-scale porosity as that of level ice also exists in the consolidated layer. A bigger scatter of the physical properties seems to be the case [Høyland et al., 2000 and this paper].

The sail porosity is often measured to be less than the keel porosity [Timco and Burden, 1997; Leppäranta and Hakala, 1992]. It is not clear why, but two reasons have been pointed out; the volume of the sail may be too small compared to the block size to get proper measurements, and the blocks in the sail may be smaller than the pieces in the keel and thereby giving more compact packing [Leppäranta et al., 1995]. It may also be that the deterioration of the keel actually increases its porosity. The measured sail porosities ranged from 21 to 24 %, which is less than the measured keel porosity (33 – 38 %).

3. Experimental

Measurements have been done on three different first-year ice ridges; Fig. 5 shows the locations. The first ridge was instrumented in 1998 and was situated off Svartodden in the Van Mijen fjord on Spitsbergen; the second was off Camp Morton in the same fjord, whereas the third was off Marjaniemi weather station on the island Hailuoto west of Oulu in Finland.

<Fig. 5>

The general meteorological and oceanographical conditions differ significantly. Therefore, it should give good basis for comparative analysis. In the Van Mijen fjord the ice usually forms in December, the melting begins from mid April (99) to mid May (98) and the ice stays until the end of June. The ice thickness reaches normally around one metre in the end of April, and the seawater salinity is about 34 ppt. Tidal currents are present in the Van Mijen fjord. The winter of 1998 was cold whereas the winter of 1999 was warm. At Marjaniemi, the ice normally forms in December or January, the melting starts in late March, and the ice is normally gone by May. The ice thickness normally reaches 0.6 m and the water salinity is from 1 to 3.5 ppt. There are practically no tide nor currents in the northern part of the Gulf of Bothnia. The winter of 1999 was a normal winter in the northern Gulf of Bothnia. The meteorological record show low pressure and strong wind around 20 January, and simulations of level ice growth predict a level ice thickness equal to the block thickness of the ridge (20 cm) around this date. This means that if the ridge was made from level ice it formed around 20 January 1999.

<<Table 1>>

Measurements of temporal and spatial temperature development, geometry, block size and structure, salinity and porosity were done on all three ridges as well as on level ice. The crystal structure of the consolidated layer was examined in the two 1999 cases, and uniaxial compression tests were done at the University of Oulu of the consolidated layer from the ridge outside Marjaniemi. The measurements are presented in Heinonen et al. [2000], Kyhring [1999], Høyland and Løset [1999a], and Langeland [1998].

Five to six thermistor-strings were installed in a cross-section of all the ridges (see Fig. 6) and one in level ice (only in 1999). The strings in the ridge were two metres apart, and had 16 temperature-sensors each. The level ice string was deployed close to the ridge and had 10 sensors. The vertical distance between the sensors was 0.1 m in the short strings, and 0.21 m for the long ones. One datalogger was attached to each string and logged the temperatures periodically as shown in Table 1. The strings, loggers, drillings equipment and procedures are described in Løset et al. [1998]. The surface was levelled, and several (3 - 5) cross-sections were drilled (2" auger) one or two times to examine geometry and porosity. Cores were taken up to measure salinity, and to make thin sections to examine crystal structure. A one metre wide channel was cut through the sail to examine the block structure. Oceanographic measurements of currents and temperatures were provided by Kangas at UNIS [Kangas, 2000]. The meteorological stations in Svea and at Marjaniemi provided weather data. In addition, a weather station was deployed 100 m away from the Svartodden ridge.

<Fig. 6>

4. Results

4.1 Geometry, morphology and porosity

The two ridges in the Van Mijen fjord were singular ridges, whereas the one at Marjaniemi was a part of a large ridged area with 3 - 6 layers of rafted ice. The Svartodden ridge had a sail height (h_s) of 1 m, the keel depth (h_k) was 4.4 m, the keel width (w_k) 10 m and the ridge was about 15 m long. The thickness of the blocks in the sail was between 0.2 and 0.25 m, and the length was between 0.5 and 1.45 m. The Camp Morton Ridge was long and curvilinear, had h_s of 1 m, h_k of 5 m, and a width of 15 m. The thickness of the blocks (h_b) in the sail was 0.10 – 0.15 m, and the length of the blocks ranged from 0.2 to 1.9 m. Visual inspection of the channels that were cut through the sail indicated that both of the Van Mijen ridges were formed in a similar way. Fig. 7 shows a drawing of a cross section at Camp Morton. It seems evident that the ice from the south was lifted and the northern part pushed down. The dates of formation for the two ridges are not known, but it is reasonable to assume that they were formed in December or January. The ridge at Marjaniemi did not have the idealised triangular shape. The sail consisted of 0.2 - 0.3 m of rafted ice and was relatively flat. The keel depth was between 4 and 5 m, and the thickness of the blocks was 0.2 m. Fig. 8 shows the same cross-section at two dates for the Marjaniemi ridge.

<Fig. 7>, <Fig. 8>

Porosity measurements were done by drilling 2" holes and registrating any drop of the drill as a pore. The keel consistence of the two ridges at Spitsbergen made it difficult to get good data for the rubble porosity. It was difficult early in the season and impossible later. At Svartodden six different cross-sections were drilled, four of them twice, altogether 93 holes. Three cross-sections were drilled at Camp Morton, two of them twice, altogether 43 holes. At Marjaniemi five cross-section were drilled, three of them twice, altogether 81 holes. Table 2 sums up the results.

<<Table 2>>

4.2 Physical properties and ice texture

The measured salinities of the consolidated layer and the level ice are shown in Tables 3 and 4. Some measurements were also done of the salinity in the sail, and the salinity of the sail was less than that of the consolidated layer. Density measurements were only done at Marjaniemi; Table 5 shows the results.

<<Tables 3, 4 and 5>>

Thin sections were made from the Camp Morton and the Marjaniemi ridges. One core was taken from the level ice in the Van Mijen (10.03.99), and two from the ridge (23.04.99 and 12.05.99). The ice from the ridge at Marjaniemi was taken 23.03.99. The level ice in the Van Mijen fjord had the regular structure with a granular layer on top and columnar ice underneath. The grain diameter was between 0.5 and 3 mm and the length of the columnar grains were up to 20 mm. The ice from the ridge showed a more irregular pattern, the grain diameter was 0.5 – 5 mm, and the length up to 20 mm. Most of the elongated grains were vertical, or close to vertical. Boundaries between either new - and old ice or two adfrozen blocks could be seen. The ice from the Finnish ridge showed the same pattern with partly granular and partly columnar ice, but the length of the columnar grains were up to 70 mm.

Uniaxial compression tests were done on the consolidated layer from the Marjaniemi ridge. The results are reported and discussed in Høyland et al. [2000], only results related to the consolidation are presented here (Table 6).

<<Table 6>>

4.3 Meteorological conditions, snow cover and level ice thickness

The heat flux out from the ice is governed by the meteorological conditions and the snow cover. One simple way of quantifying the amount of cold that is taken away from the ice is *the cumulative freezing degree-days FDD:*

$$FDD = \int_{t_0}^{t} \left(T_f - T_{air}\right) dt, \qquad \left(T_f - T_{air} \geq 0\right) \tag{2}$$

where T_f is the freezing temperature of the water, T_{air} the air temperature and t-t_0 is the time period of interest.

Tables 7 and 8 show *FDD's* and snow conditions. Some care should be taken in comparing *FDD's* for different latitudes because the influence of the solar radiation is not incorporated in the *FDD*-expression. The solar radiation is more important on Spitsbergen because part of the growth season takes place after the vernal equinox.

<<Table 7 and 8>>

The thickness of the level ice was measured manually and with thermistor-strings (not for the Svartodden case). Table 9 sums up the measurements. The freeboard was about zero for the two Van Mijen ridges, and superimposed ice was formed. Off Marjaniemi, the freeboard was all the time positive (3 – 5 cm).

>>Table 9>>

4.4 Consolidation, keel consistence and oceanographical conditions

Table 10 displays some key features from the measurements of consolidation such as the growth of the consolidated layer (Δh_c), its relation to the growth of the level ice ($\Delta h_c / \Delta h_i$), the growth of the consolidated layer per day ($\Delta h_c / day$), the average final thickness of the consolidated layer (h_c), its relation to the final thickness of the level ice ($R_{avg} = h_c / h_i$), the ratio of the maximum thickness of the consolidated layer to the final thickness of the level ice ($R_{max} = h_{c,max} / h_i$) and the duration of the growth. In Fig. 9 R_{avg} is plotted against the ratio of the level ice thickness to the block thickness (h_i/h_b). Only manual level ice thickness measurements are used in this figure. Table 11 summarizes the keel consistence and some oceanographical condition.

>>Table 10>>

<Fig. 9>

<<Table 11>>

Measurements of water temperatures have been done by Kangas [2000]. He found that the temperatures in the water-masses were homogenous around the freezing point in the fjord in late March 1998, and that an intrusion of warm coastal-water (up to T = -1.6°C) entered the fjord by late April 1999. Temperatures were measured in ice cores from the Camp Morton ridge 12.05.99. The partly consolidated layer had a temperature of –1.6°C whereas the temperatures in central parts were about –1.9°C.

5. Results from the literature

Table 12 summarizes some results from the literature about ridge consolidation. It is not meant to be a complete review, but it is the published results the author is presently aware of. The relationship between the consolidated layer and the level ice concerning absolute size or growth seems to be in-between 1.2 and 1.9 for all. Beketsky [1998] reports of ridge measurements from the Sea of Okhotsk. In the ridges that were 3 months old, they found average values of the thickness of the consolidated zone of about 3.5 m, and porosity ranging from 15 – 28 %. The thickness of level ice is not given in the paper.

<<Table 12>>

Special attention will be paid to the work done by Timco and Goodrich [1988]; it elucidated some important aspects of the initial phase of a consolidation process. Ice sheets were grown in the laboratory and at a certain thickness ($h_{i,0}$) rubble was made from parts of the ice cover. Thermistor-strings were installed in the rubble, and temperatures as well as visual inspection were used to estimate the thickness of the consolidated zone. The rubble was left to consolidate for a while before the ridge was destroyed and inspected. At the end of each test the thickness of the consolidated layer ($h_{c,f}$) and the final level ice thickness ($h_{i,f}$) were measured. The temperature measurements generally gave a thinner layer. A ratio of the thickness of the consolidated zone, estimated by respectively temperatures and visual inspection was 0.79. In the following, we are only referring to the temperature derived thicknesses. In Fig. 10 the two ratios –the thickness of the consolidated layer divided by the level ice growth ($h_{c,f}/\Delta h_i$) and – the thickness of the consolidated layer divided by the level ice thickness (R_{avg}) are plotted against the growth of the level ice during the consolidation process (Δh_i). Either of these ratios seems to decrease with increasing level ice growth during consolidation. This decrease also decreases with increasing time for the former of these ratios, but seem to stabilize after a while. The importance of Fig. 10 is that it clearly demonstrates the effect of the internal redistribution of heat during the initial phase. When the temperatures even out in the keel the heat transfer upwards becomes the dominating process and the growth rate decreases. Table 13 shows that the longest lasting of Timco and Goodrich' tests corresponds well with the fieldwork presented in this paper. Results from experiments with laboratory made ridges in HSVA in Hamburg by Jensen et al. [2000] fits well into Fig. 10.

<<Table 13>>

<Fig. 10>

6. Discussion

6.1 Geometry, morphology and porosity

The two Van Mijen ridges were small or medium arctic ridges. The block thickness indicates that they were formed during one event. It is also probable that they were created from level ice, but this is not certain. The keel depth to sail height ratios correspond well with Timco and Burden [1997]. As described in Section 3.1 it looked like one ice sheet has been pressed up and the other bent down. This has also been found by Tukhuri et al. [1999]. The Marjaniemi ridge was part of a large ridge area and did not have the typical triangular shape. This kind of ridged ice feature is not rare outside Marjaniemi, although it was less rafted ice and more singular ridges the previous and the following years.

The measurements of porosity correspond well with results from the literature (Table 12). None of these authors has reported any value on porosity of the consolidated layer. The sail porosity is as expected less than the keel porosity.

6.2 Physical properties and ice texture

The salinity and density values presented in Section 4.2 are comparable to what others have found (Table 12). The measurements presented by Høyland and Løset [1999b] where salinity in neighbouring ridges of varying age was found to differ significantly (4 - 29 ppt) suggest that brine is drained quite efficiently and stabilises on what is found in level ice. The scatter of the physical properties of the consolidated layer was almost exclusively higher than for the level ice. The number of samples was limited but it is still an indication that the consolidated zone is a more inhomogeneous material than the level ice. If this also applies for mechanical properties, it is important for attempts to find mechanical strength and forces applied by ridges on structures in ridge-structure interaction. The relatively short grains in the Van Mijen fjord was due to the under-ice currents breaking the needles and disturbing the crystal formation [Eicken et al., 1998].

6.3 Meteorological conditions, ice growth and the snow cover

The meteorological conditions around the three ridges differed significantly. The cold winter of 1998 resulted in ice growth in the Van Mijen fjord until mid May, whereas it stopped at the end of April in 1999. Less snow and a higher growth rate were measured at Marjaniemi. The non-symmetrical snowdrift early in the season gave a corresponding non-symmetrical consolidated zone for the two Van Mijen ridges. These observations stress the importance of the insulating effect of the snow cover. There is some discrepancy between the level ice thickness measured manually and by temperatures (see Table 9). This may be explained by the resolution of the thermistor-strings, or by an uneven ice cover (the thickness measurements were not done at the exact same spot each time). In the Van Mijen fjord, the discrepancy was probably due to superimposed ice. The freeboard was little in both cases, and the ice was flooded occasionally when holes were made. The spring of 1999 the formation of 5 cm of superimposed ice was measured. The salinity measurement performed 25.04.98 also indicate that superimposed ice was formed here. However, we do not know how much, but the following short argument may give an indication. As long as there are cracks in the ice so that it can be flooded, and there is sufficient precipitation, the ice thickness determines the formation of superimposed ice. A thicker ice cover can take more snow without being submerged. Therefore, with the same amount of precipitation and the same snow density a thinner ice cover gives more superimposed ice and a thinner snow cover. The relationship between the level ice thickness for the two seasons in the Van Mijen fjord corresponds to the measured snow thicknesses. This indicates that less superimposed ice may have been formed in 1998. As the freeboard was all the time positive outside Marjaniemi, there is reason to believe that little superimposed ice was formed.

6.4 Deterioration of the keel and oceanic flux

Table 11 shows that a marked difference in the consistence of the keel was found between the ridges at Spitsbergen and the one in the Gulf of Bothnia. Three possible reasons can explain this discrepancy: a) Salinity, b) Velocity and temperature of surrounding currents and c) Exposed area to volume ratio. These three factors indicate a more effective internal redistribution of heat and higher oceanic flux on Spitsbergen. The relative contribution of the two fluxes to the deterioration of the keel is not clear. The internal redistribution of energy is a complex process including internal flow due to variations in density, salinity and temperature as well as melting and formation of ice crystals. There are several indicators of seasonal variations in the oceanic flux in the Van Mijen fjord. The measurements of Kangas [2000], and our own measurements of warm ice under the consolidated layer late in the season indicates no flux in the cold season and some flux in the melting period. The ridge keel temperatures in an instrumented stamucha in the Van Mijen fjord in 1997 showed that it was heated from below as well as from above in late May and June. Temperatures up to –0.6°C was recorded in the lower parts of the keel. The lowest temperatures could be found in the middle of the keel [Løset et al., 1998]. Finite element simulations of ice growth in the Van Mijen fjord also suggests zero flux during the growth period [Høyland, 2000]. This does not mean that there is no energy transfer between the ice in the keel and the surrounding water. If there are some currents present, and there is some permeability in the keel is it reasonable to expect that there will be some mechanical and thermal erosion.

6.5 The consolidated zone

Examination of Table 10 reveals an important distinction. The three top rows comprise figures related to the growth of the consolidated layer, and in the three subsequent ones are values related to the total thickness of the consolidated layer. In the latter case, it seems to be a systematic difference between the numbers derived from temperature measurements and the ones obtained from drillings. The temperature measurements predict a thinner consolidated zone. An average ratio, h_c^T/h_c^D for the three ridges is 0.78. This difference cannot be found in the three top rows. Drilling results are generally more uncertain because they rely more on the person operating the drill. However, there is no reason to believe that this uncertainty should result in a systematic overestimation. Two reasons may be pointed out to explain this difference:

1. The given temperature derived data are minimum values
2. The drilling results include a partly consolidated layer.

Explanation number one is not sufficient to explain the difference; even if the vertical resolution of the thermistorstring (0.21 m) is added to h_c^T it does not reach the value of h_c^D, there is a still a ratio of h_c^T/h_c^D of 0.94. Timco and Goodrich [1988] and Veitch et al. [1991c] also found that the temperature estimates of the thickness of the consolidated layer were lower than what was found in a visual inspection (h_c^T/h_c^D = 0.79 and 0.92 respectively). A better examination of the mechanical definition of the consolidated layer such as the compression tests presented in Table 6, is seen to correspond well with the temperature-derived values. It is generally more difficult to compare drilling results than temperature measurements and standardised mechanical testing. However, it looks as if the partly consolidated layer is easily incorporated in the estimate of the consolidated layer by drilling.

The ridge examined by Leppäranta et al. [1995] was also situated off the Marjaniemi weather station and their results are similar to ours. Their higher growth rate corresponds with lower porosity; a higher final value for R_{avg} in our case is probably due to the rafted layers that gave a higher initial growth rate. In general the results presented in Tables 10 and 12 correspond well, the thickness of the consolidated layer has been found to be less than two times the thickness of the level ice for all ridges.

If the effect of delayed response due to thermal inertia is excluded, the growth rate $\Delta h_c / \Delta h_i$ follows the vertical variation of porosity. The growth rate governs the development of R_{avg}. In Fig. 9 it can be seen that the R_{avg} increased with time in all the field measurements [also Leppäranta et al., 1995], approaching a value of about 1.5 for the temperature measurements and 1.8 for the drilling results. The relatively low initial value (1.06) for the Marjaniemi ridge can be explained by its young age at the time of instrumentation. The low R_{avg} found by Coon et al. [1995] is probably also due to low a ridge age. An interesting difference between laboratory work [Timco and Goodrich, 1988] and fieldwork becomes evident when examining Fig. 10 and Fig. 9. Whereas R_{avg} increases with time in Fig. 9, it decreases in Fig. 10 and approaches the temperature given field values (Table 13). This indicates that the initial thickness of the consolidated zone in laboratory made ridges is overestimated. It may be due to a problems with scaling and/or smaller initial oceanic flux in a basin than what exists in the real world.

The warm winter of 1999 at Spitsbergen resulted in a thinner consolidated zone, a shorter duration of growth and a smaller average growth per day than what was the case in 1998. The ridge at Marjaniemi had a higher growth per day; this is probably due to less insulation caused by a thinner snow cover.

6.6 Some comments about uncertainty

Table 10 presents the most important results in this article. However, it is important to keep in mind that the given values are derived from the measurements. This means that there is a number of assumptions in-between e.g. the temperature measurements and the temperature derived thickness of the consolidated layer (h_c^T). The measurements itself, and the derivation of results both constitute uncertainty. Let us focus on the following two aspects: 1) that the given h_c^T is an average of the thermistor-strings of a cross-section and 2) the resolution of the thermistor-strings and its relation to the drillings.

Firstly, the averaging of the thermistor-strings in a cross-section. If only the three "coldest" thermistor-strings are used to calculate h_c^T for the two Van Mijen ridges, the result would be as follows: Svartodden h_c^T=1.85, Δh_c=0.50 and R_{avg}=1.60, and Camp Morton h_c^T=1.21, Δh_c=0.21 and R_{avg}=1.72. Little difference would be found in the Marjaniemi ridge. Secondly, the resolution of the thermistorstring and manual thickness measurements. Table 14 presents some extreme values for R_{avg} when the resolution of the strings and the discrepancy between the manual level ice thickness measurements and the ones obtained from the thermistor-strings are considered.

<<Table 14>>

6.7 Analytical solutions

Two analytical solutions based on the assumptions behind Stefan's law are presented. The first gives the thickness of the consolidated layer and the second the relation between the growth of the consolidated layer and the growth of the level ice.

The heat transfer equation governs conductive heat transfer in any material. This equation becomes with certain simplifications [see e.g. Leppäranta, 1993] the well known Stefan's law. If one further introduces an empirical coefficient ω to account for these simplifications the thickness of an ice sheet can be calculated according to the following formula:

$$h^2(t) = h_0^2 + \omega \frac{2k}{\rho \cdot l} \int_{t_0}^{t} \left(T_f - T_{air}\right) dt \tag{3}$$

where $h(t)$ is the present ice thickness, h_o the initial ($t=t_0$) thickness, T_f is the freezing temperature of the water, T_{air} the air temperature, k the thermal conductivity, ρ the density and l the latent heat of ice. The integral expression (*FDD*) is defined in Eq. (2).

When a ridge consolidates, only parts of the volume need to change phase. Stefan's law can be adjusted for freezing of rubble by assuming that the latent heat is reduced by multiplying with the porosity of the rubble that is about to freeze [Leppäranta and Hakala, 1989]:

$$l_r = \eta \cdot l_{pi} \tag{4}$$

where l_r is an 'effective' latent heat of fusion for the rubble, η the macro porosity and l_{pi} is the latent heat for pure ice.

If Eqs. (3) and (4) are combined an expression for the 1-D freezing of rubble is obtained. If the same ω yields for the growth of the consolidated layer, the thickness of this layer as a function of the level ice thickness and porosity can be derived:

$$h_c^2(t) = h_{c,0}^2 + \frac{h_i^2(t) - h_{i,0}^2}{\eta} \tag{5}$$

The second model is presented in Høyland [2000] and relates the growth of the consolidated layer to the growth of the level ice, R_{avg}, and the total porosity:

$$\frac{dh_c}{dh_i} = b\frac{l_i}{l_r} \cdot \frac{h_i}{h_c} = \frac{b \cdot l_i}{l_r \cdot R_{avg}} \tag{6}$$

where b is a constant to adjust for a possible difference in insulation, l_i and l_r are the latent heats of the level ice and the rubble respectively and h_i and h_c are the thicknesses of the level ice and the consolidated layer.

This equation states that the growth rate in the rubble relative to the growth rate in seawater basically is a function of the relation between the latent heats (i.e. the porosity) and the relative thickness of the consolidated layer to the level ice thickness.

Some calculations using the two models are presented in Tables 15 and 16. Predictions of the thickness of the consolidated layer by Eq. (5) and the coefficient ω in Stefan's law are given in Table 15. The ω found from the Marjaniemi ridge corresponds with values for the Gulf of Bothnia [Leppäranta and Hakala, 1992]. At Spitsbergen, the coefficient was lower due to the thicker snow cover and the solar radiation. The snow cover insulates and prevents the cold weather to subtract heat from the ice. The solar radiation is not incorporated into the *FDD* expression, but is important to the thermal balance as it adds energy to the ice. Generally, the adjusted Stefan's law fits the measurements reasonably well. However, it is not clear how to treat the superimposed ice.

<<Table 15>>

If we assume that R_{avg} approaches dh_c/dh_i, a limit value can be found from Eq. (6). Table 16 presents some limit values as a function of l_r (l_i=0.85l_{pi} and b=1). If R_{avg} initially is less than the limit it will increase and approach the limit. In this case, Table 16 gives maximum limits for the thickness of the consolidated layer divided by the level ice thickness. However, R_{avg} may also decrease, as seen in Fig. 10. Table 16 then displays minimum values.

<<Table 16>>

The limit values for our three ridges becomes about 1.8, and this is higher than what was measured. However, the measured growth rate ($\Delta h_c/\Delta h_i$) relative to the measured R_{avg} correspond with the equation. Thus, more time was needed if the limit value should have been reached. It is important to keep in mind that these analytical models contain several simplifications. The thermal inertia and the oceanic flux are neglected, and it is assumed no spatial or temporal development of the porosity. Due to thermal inertia there will be a delayed response in a thicker compared to a thinner ice feature. Thus, fluctuations and not monotonically increase/decrease may be found in the real world. The oceanic flux adds heat to the ridge and from this point of view it only contributes to decrease the growth. Nevertheless, if the deterioration of the keel leads to a rearrangement or gradually collapse of the keel structure, the keel porosity is affected. It may decrease and thus increase the growth rate. Spatial variations in keel porosity have been found. Lensu [1993] describes a mid-keel minimum in porosity.

If this is to be used as a background for design of structures, the question of increase or decrease of R_{avg} becomes crucial. Fig. 9 shows that the four in-situ ridges confessed to increase, whereas the laboratory example given in Fig. 10 decreased. Let us highlight two important points that should be investigated in order to clarify the question of increase or decrease and maximum values: 1) try to understand the initial phase of consolidation better. Especially the effect of the initial temperature of the ice blocks and, 2) to examine spatial and temporal development of keel porosity quantitatively. As design has to consider the worst case, statistics are necessary. The work of Beketsky et al. [1997 and 1998] seems to represent an extreme case concerning consolidation (low η and high h_c) and should be of special interest.

7. Conclusions

Three different ice ridges have been examined to gain increased insight in the effects of consolidation. The thickness of the consolidated layer has been examined in three ways, by temperature measurements, by drilling and in one case by uniaxial compression tests. The geometry, porosity and physical properties of the ridge and of the level ice have also been measured. Two analytical solutions are presented; one to estimate the growth of the consolidated layer and one for its size. They are both based on Leppäranta and Hakalas [1989] modifications of Stefan's law. The major findings of this paper are the following:

- The temperature measurements gave a ratio R_{avg} = 1.39 - 1.61, the drillings gave R_{avg} = 1.68 - 1.85. The average ratio for the three ridges, h_c^T / h_c^D was 0.78 (minimum temperature values), or 0.94 (maximum temperature values).
- The compression tests corresponded well with the temperature definitions of the consolidated layer.
- The method of investigation affects the result. Mechanical drillings seems to overestimate the thickness of the consolidated layer.
- The growth of the consolidated layer did not depend on the method of investigation.
- The scatter of the physical properties of the consolidated layer was higher than that of the level ice.
- Brine seems to drain efficiently from the consolidated layer and stabilise on what can be found in level ice.
- The difference in keel consistency between the ridge at Marjaniemi and the ones in the Van Mijen fjord can be explained by differences in salinity, surrounding currents and exposed area/volume ratio for the keels.
- The consolidation process can be divided into 1) an initial phase in which the internal redistribution of energy and the heat transfer from the ocean is crucial and 2) a main phase where the keel-temperatures are equal to T_f and the dominating heat flux goes up into the cold surrounding air.
- Leppäranta and Hakala's [1989] modification of Stefan's law fits the measurements well. However, it is not clear how to treat superimposed ice.
- The rate of the growth of the consolidated layer divided by the growth of the level ice depends on the porosity and R_{avg} in such a way that the effect of the porosity decreases with increasing R_{avg}. An equilibrium value can be found.

Acknowledgement

The author would like to thank siv.ings Arne Langeland, Morten Kyhring and Guro Kjestveit for their crucial assistance in the fieldwork. The University Courses on Svalbard and the Norwegian Research council gave financial support to the work. Very important have also been dr.student Jaakko Heinonen and professor Mauri Määttänen from Helsinki University of Technology (HUT) who led the field program in Finland. The fieldwork in Finland was a part of the LOLEIF project in the framework of the EU-sponsored Marine Science and Technology (MAST-III). Programmed under contract no. MAS3-CT97-0078. The author is grateful for financial support and valuable discussion. The Norwegian Research Council paid my salary for three year something, which is appreciated highly. I am also thankful to my colleague Arnor Jensen for many fruitful discussions over the past two years. He also read this manuscript and is responsible for several improvements. Finally, I would like to thank my supervisor professor Sveinung Løset for participation in the field-work, never-ending enthusiasm, encouragement and discussions.

References

Ashton, G.D. (ed.) 1986. River and lake ice engineering, Book Crafters Inc., Michigan,USA, ISBN 0-918334-59-4, pp. 47-48.

Beketsky, S.P. Thickness distribution of consolidated hummock layer offshore Sakhalin. Proceedings of the 14th International Symposium on Ice (IAHR), Potsdam, New York, USA, 27-30 July, Vol. 1, pp. 357-359, 1998.

Beketsky, S.P., Astafiev, V.N. and Truskov, P.A., Design parameters for hummocks and grounded hummocks in the Sea of Okhotsk. Proceedings of the International Offshore and Polar Engineering Conference (ISOPE), Honolulu, USA, 25-30 May, Vol. 2, pp. 487-493, 1997.

Coon, M.D., Douglas, C.E. and Gerald, S.K., Force displacement measurements of a first-year pressure ridge keel. ASME, Ice mechanics, AMD-Vol. 207, pp. 239-254, 1995.

Cox, G.F.N. and Weeks, W.F., Equations for determining the gas and brine volumes in sea-ice samples. Journal of Glaciology, Vol. 29, No. 102, pp. 306-316, 1983.

Croasdale, K.R., Allen, N.F.B. and Marcellus, R.W., Thermal response of ice rubble: predictions and observations. Proceedings of the 10th International Symposium on Ice (IAHR), Espoo, Finland, 20–24 August, Vol. 1, pp. 153-167, 1990.

Eicken, H., Weissenberger, J., Bussmann, I., Freitag, J., Schuster, W., Valero Delago, F., Evers, K.-U., Jochmann, P., Krembs, C., Gradinger, R., Lindemann, F., Cottier, F., Hall, R., Wadhams, P., Reisemann, M., Kousa, H., Ikävalko, J., Leonard, G.H., Shen, H., Ackley, S.F. and Smedsrud, L.H., Ice-tank studies of physical and biological sea-ice processes. Proceedings of the 14th International Symposium on Ice (IAHR), Potsdam, New York, USA, July 27-31, Vol. 1, pp. 363-370, 1998.

Frederking, R.M.W. and Wright, B., Characteristics and stability of an ice-rubble field Issungnak, February-March 1980. NRC Technical memorandum,, No. 134, pp. 230-247, Jan 1982.

Granberg, H.B., Snow cover on sea ice. In: The physics of ice covered seas, lecture notes from a summer school in Savonlinna, Finland, 6-17 June 1994, ISBN 951-45-8226-8, Vol. 2, pp.605-649, 1998.

Heil, P., Allison, I. and Lytle, V.I., Seasonal and interannual variations of the oceanic heat flux under a landfast Antarctic Sea ice cover. Journal of Geophysical Research, Vol. 101, No. C11, pp. 25741-25752, 1996.

Heinonen, J., Määttänen, M., Høyland, K.V. and Kjestveit, G., Ridge load experiments, field experiments in winter of 1999. Unpublished LOLEIF report, 73 p, 2000.

Høyland, K.V. Simulations of the consolidation process in first-year ice ridges, Submitted to the Journal of Cold Region Science and Technology.

Høyland, K.V., Kjestveit, G., Heinonen, J. and Määttanen, M., LOLEIF ridge experiments at Marjaniemi: The size and strength of the consolidated layer. Proceedings of the 15th International Symposium on Ice (IAHR), Gdańsk, Poland, 28 August-1 September, Vol. 1, pp. 45-52, 2000.

Høyland, K.V. and Løset, S., Measurements of temperature distribution, consolidation and morphology of a first-year sea ice ridge. Cold Regions Science and Technology 29 (1999), pp. 59-74, 1999a.

Høyland, K.V. and Løset, S., Monitoring and observation of the formation of a first-year ice ridge-field. Proceedings of the 15th International Conference on Port and Ocean Engineering under Arctic Conditions, Espoo, Finland 23–27 August 1999, Vol. 1, pp. 37-48, 1999b.

Jensen, A., Høyland, K.V. and Evers, K.-U., Scaling and measurements of laboratory made rubble. Proceedings of the 15th International Symposium on Ice (IAHR), Gdańsk, Poland, 28 August-1 September, Vol. 1, pp. 105-112, 2000.

Kangas, T-V. 2000 Thermihaline sesongvariasjoner i Van Mijen fjorden (in Norwegian). Cand Scient Thesis in Oceanography at the University of Bergen / the University Courses on Svalbard (UNIS), 73 p, 2000.

Kankaanpää, P., Distribution, morphology and structure of sea ice pressure ridges in the Baltic Sea. Fennia 175:2, pp 139-240. Helsinki. ISSN 0015-0010, 1997.

Krankkala, T. and Määttänen, M., Methods for determining ice forces due to first- and multi-year ridges. Proceedings of the 7th International Symposium on Ice (IAHR), Hamburg, Germany 27-31 August, Vol. 4, pp. 263-287, 1984.

Kyhring, M., Thermo-mechanical properties of a first-year ice-ridge. Engineering diploma thesis at the University Courses on Svalbard (UNIS) / the Norwegian University of Science and Technology (NTNU), 40 p, 1999.

Langeland, A., Measurements of geometry and temperature distribution of pressure ridges on Svalbard. Engineering diploma thesis at the University Courses on Svalbard (UNIS) / the Norwegian University of Science and Technology (NTNU), 40 p, 1998.

Lensu, M., Ice morphology. In: Pekka Kosloff & Mikko Lensu, Matti Leppäranta, Pekka Pihkala, Markku Similä (eds.) BEERS 92 R/V Aranda Base data report II: the measurements. Finnish Institute of Marine Research. Internal Report 5, pp. 15-51, 1993.

Leppäranta, M., Lensu, M., Koslof, P. and Veitch, B., The life story of a first-year sea ice ridge. Cold Regions Science and Technology, 23 (1995), pp. 279-290, 1995.

Leppäranta, M., A review of analytical models of sea-ice growth. Atmosphere-Ocean 31 (1) 1993, pp 123-138, 1993.

Leppäranta, M. and Hakala, R., The structure and strength of first-year ridges in the Baltic Sea. Cold Regions Science and Technology, 20, pp. 295-311, 1992.

Leppäranta, M. and Hakala, R. 1989. Field measurements of the structure and strength of first year ice ridges in the Baltic Sea. Proceedings of the 8th International Conference on Offshore Mechanics and Arctic Engineering (OMAE), The Hague, the Netherlands, Vol. 4, pp. 169-174.

Lytle, V.I. and Ackley, S.F., Heat flux through sea ice in the western Weddell Sea: convective and conductive transfer processes. Journal of Geophysical Research, Vol. 101, No. 94, pp. 8853-8868, 1996.

Løset, S. 1992. Heat exchange at the air surface of icebergs. Proceedings of the 11th International Symposium on Ice (IAHR), Banaff, Alberta, Canada, pp. 735-746.

Løset, S., Langeland, A., Bergheim B. and Høyland, K.V., Geometry and physical properties of a stamucha found on Spitsbergen. Proceedings of the 14th International Symposium on Ice (IAHR), Potsdam, New York, USA, 27-31 July, Vol. 1, pp. 339-344, 1998.

Maykut, G.A. 1986. The surface heat and mass balance. In 'The geophysics of sea ice', edited by N.Untersteiner pp. 395-463.

Maykut, G.A. and Perovich, D.K., The role of short-wave radiation in the summer decay of a sea ice cover. Journal of Geophysical Research, Vol. 92, pp. 7032-7044, 1987.

Mironov, Y.U., Poplin, J.P., Wang, A.T., Klyachkin, S.V. and Speransky, D.A., Winter 1998 study of ice ridge geometry offshore Sakhalin island. Proceedings of the 15th International Conference on Port and Ocean Engineering under Arctic Conditions, Espoo, Finland 23 –27 August, Vol. 1, pp. 60-69, 1999.

Parmerter, R.R. and Coon, M.D., On the mechanics of pressure ridge formation in sea ice. Offshore Technology Conference, paper number OTC 1810. 6200 North central Expressway, Dallas, Texas 75206, USA, 1973.

Parmerter, R.R. and Coon, M.D., Model of pressure ridge formation in sea ice. Journal of Geophysical Research, Vol. 77, No. 33, pp. 6565-6575, 1972.

Timco, G.W., Wright, B., Johnston, M. and Frederking, R., First-year ice ridge loads on Molikpaq. Proceedings from the 4th International Conference on Development of Russian Arctic Offshore (RAO), St. Petersburg, Russia, 6 –9 July 1999, Vol. 2, pp. 172-179, 1999.

Timco, G.W. and R.P. Burden, An analysis of the shapes of sea ice ridges. Cold Regions Science and Technology, Vol. 25, pp. 65-77, 1997.

Timco, G.W. and Goodrich, L.E., Ice rubble consolidation. . Proceedings of the 9th International Symposium on Ice (IAHR), Sapporo, Japan, pp. 426-438, 1988.

Tuhkuri, J., Lensu, M. and Saarinen, S., Laboratory and field studies on the mechanics of ice ridge formation. Proceedings of the 15th International Conference on Port and Ocean Engineering under Arctic Conditions, Espoo, Finland 23 –27 August 1999, Vol. 3, pp. 1118-1129, 1999.

Veitch, B., Lensu, M., Riska, K., Kosloff, P., Keiley. P. and Kujala, P., Field observations of ridges in the northern Baltic Sea. Proceedings of the 11th International Conference on Port and Ocean Engineering under Arctic Conditions, St. John's, Canada, pp. 381-400, 1991a.

Veitch, B., Kujala, P., Kosloff, P. and Leppäranta, M., Field measurements of the thermodynamics of an ice ridge. Report M-114, Laboratory of Naval Architecture and Marine Engineering, Helsinki University of Technology, Espoo, Suomi, 53 p, 1991b.

Veitch, B., Kujala, P, Keiley. P. and Lehmus, E., Ice tank experiments on the thermodynamics of deformed ice. Report M-110, Laboratory of Naval Architecture and Marine Engineering, Helsinki University of Technology, Espoo, Suomi, 46 p. ISBN 951-22-0655-2, ISSN 0784-5650, 1991c.

Figure captions

Fig. 1. A ridge in the Van Mijen fjord on Spitsbergen (photo taken by Bjarne Bergheim).

Fig. 2. A ridge in front of the Tuna glacier in the Tempelfjord on Spitsbergen March 1998 (photo taken by Stian Soltvedt).

Fig. 3. Illustration of the different fluxes and heat transfer mechanisms in an ice ridge.

Fig. 4. Typical temperature and salinity profile in young sea ice.

Fig. 5. Map of the sites.

Fig. 6. Thermistor-strings in the ridge outside Camp Morton.

Fig. 7. Sketch of the structure of the sail in the Camp Morton ridge

Fig. 8. Cross-section of the ridge at Marjaniemi. The grey area is the keel, the white the sail, the dotted white is the snow and the black dots are the pores: a) 26.02.99 b) 25.03.99

Fig. 9. R_{avg} versus the ratio of the level ice thickness to the block thickness.

Fig. 10. Timco and Goodrich's (1988) laboratory work, the line with triangles is R_{avg} and the line with squares is $\Delta h_c/\Delta h_i$.

Table 1. Description of the three sites.

	Svartodden (Spitsbergen)	Camp Morton (Spitsbergen)	Marjaniemi (Finland)
Latitude	77.5º N	77.5º N	65º N
Instrumented period	2 March – 12 May 1998	10 March – 5 May 1999	25 Feb. – 25 March 1999
Type of ridge	Short linear single ridge	Long curvilinear single ridge	Large rafted ridge-field

Table 2. The measured porosity in the three ridges (%).

	Svartodden	Camp Morton	Marjaniemi
Sail	24 (93 holes)	-	21 (6 holes)**
Cons. + partly cons.	3.4 (93 holes)*	-	-
Rubble	33 (4 holes)	35 (uncertain)	38 (81 holes)

*Most of these pores were found close to the rubble, mostly in the partly consolidated layer.

**The drilling was done in a nearby sail, less than 200 m from the thermistor-strings

Table 3. The salinity of the consolidated and partly consolidated layer.

	Svartodden			Camp Morton		Marjaniemi
Date	25.03	28.04	28.04	23.04	12.05	23.04
Average (ppt)	5.4	4.41	4.71	4.48	3.77	0.24
St.dev (ppt)	2.61	1.54	0.76	2.90	0.79	0.10
Maximum (ppt)	10	6.5	6	11.6	5.80	0.38
n (-)	5	16	7	10	12	6

Table 4. The salinity of the level ice.

	Svartodden		Camp Morton		Marjaniemi
Date	18.04	25.04*	08.05	14.05	23.03
Average (ppt)	5.64	5.33 / 4.5	3.07	2.88	0.42
St.dev (ppt)	0.94	2.60 / 0.76	1.34	0.91	0.14
Maximum (ppt)	7	12 / 7	5.86	4.63	0.5
n (-)	7	9 / 8	8	8	4

* The sample from the top of the ice had a salinity of 12 ppt, this was probably because of flooding. The first set of numbers includes these measurements, and the second does not.

Table 5. The density measurements at Marjaniemi (23.03.99 and 24.03.99).

	Consolidated layer		Level ice	
	Drained	Undrained	Drained	Undrained
Average (kg/l)	0.83	0.90	0.89	0.89
St.dev (kg/l)	0.06	0.03	0.02	0.01
Maximum (kg/l)	0.88	0.97	0.90	0.89
n (-)	7	7	4	4

Table 6. The uniaxial compression tests of the consolidated layer in the Marjaniemi ridge.

	Depth below the water line (cm)						
	-15 – 5	5 - 25	25 – 45	45 – 65	65 - 85	85 - 105	105 – 125
σ_c (MPa)	5.0	5.2	7.2	6.2	4.8	1.5	1.7

Table 7. Meteorological conditions.

		Svartodden	Camp Morton	Marjaniemi
Instrumented period	Duration (weeks)	10	8	4
	FDD (°C days)	985	680	134
Growth period	Duration (weeks)	10	7	3
	FDD (°C days)	985	620	126
Characterisation		Cold	Warm	Normal

Table 8. The snow conditions (m).

	Svartodden	Camp Morton	Marjaniemi
Maximum snow depth on level ice	0.4	0.3	0.05
Snow drift around the ridges	0-0.9	0-0.8	0.05-0.15

Table 9. The thickness of level ice (m).

	Svartodden	Camp Morton		Marjaniemi	
Method	Manual	Manual	Temp.	Manual	Temp.
$h_{i,0}$	0.95	0.70	0.6 – 0.7	0.47	0.4 –0.5
$h_{i,f}$	1.16*	0.85	0.7 – 0.8	0.60	0.5 – 0.6
Δh_i	0.21	0.15**	0.1	0.13	0.1

*2 cm increase in freeboard

**5 cm of superimposed ice

Table 10. Key features of consolidation for the three ridges. Minimum values are used for the temperature-derived h_c.

	Svartodden		Camp Morton 99		Marjaniemi 99	
	Temp.*	Drillings (93 holes)	Temp.	Drillings** (43 holes)	Temp.	Drillings (81 holes)
Δh_c (m)	0.42	0.40	0.22	0.30	0.21	0.23
$\Delta h_c / \Delta h_i$	2.0	1.9	2.2	2.0	2.0	1.75
$\Delta h_c / day$ (cm/day)	0.60	0.57	0.45	0.61	1.00	1.02
h_c (m)	1.61	1.95	1.13	1.35	0.71	1.03
$R_{avg} = h_c / h_i$	1.39	1.68	1.61	1.60	1.42	1.85
$R_{max} = h_{c,max} / h_i$	1.84	2.37	2.14	2.17	1.72	-
Duration of growth	10 weeks		7 weeks		3 weeks	

*At Svartodden did we not get data from the level ice string, so the values of level ice thickness are from drilling, this gives a higher value than a temperature string does, so the values for R_{avg} and R_{max} may be a little low. The central string failed in Svartodden and was not replaced until week 16.

**At Camp Morton did we not perform so much drilling as in the two other cases, so the values from the drilling results are less reliable in this case.

Table 11. General keel conditions.

	Svartodden	Camp Morton	Marjaniemi
Rubble consistence	Soft	Soft	Harder
Porosity measurements	Difficult, impossible late in the season	Difficult, impossible late in the season	Easy, also late in the season
Water salinity (ppt)	34	34	1-3.5
Assumed age at instrumentation	2 months	2 months	1 month
Surrounding currents	Tidal currents	Tidal currents	Little
Exposed area / keel volume (m^2/m^3)	0.65	0.67	0.25

Table 12. Summary of ridge experiments. ^{T} and ^{D} refer to whether temperatures or drillings have been used.

	R_{avg}	$\Delta h_c/\Delta h_i$	Field / lab	Ridge age (days)	Salinity (ppt)	Porosity (%)	Density (kg/l)
Coon et al.	1.24 ^{D}	1.87 ^{D}	Field	15	4.4 – 5.4	25 –35	-
Croasdale et al.	1.6	-	Lab.	18	-	-	-
Frederking and Wrigth	1.75 ^{D}	-	Field, grounded	-	3 – 5	30	-
Kankaanpää	1.42 ^{D}	-	Field	-	0.3 – 0.8	30	0.8 – 0.9
Leppäranta et al.	1.75 ^{D}	1.85 ^{D}	Field	87	0.2 – 0.3	32	-
Veitch et al. (a and b)	1.25 ^{T}	1.54 ^{T} / 1.35 ^{D}	Field		0.2 – 0.7	32	0.907
Veitch et al. (c)	1.98 ^{T} / 2.13 ^{V*}		Lab.	3 – 4		35 - 47	

*Visual inspection of the ridges after each test was used to estimate the thickness of the consolidated layer.

Table 13. h_c / Δh_i and R_{avg} for the three in-situ measurements and one of Timco and Goodrich' laboratory tests (temperature based).

	Svartodden 98	Camp Morton 99	Marjaniemi 99	Timco and Goodrich 88
h_c / Δh_i	1.76	1.88	1.78	1.79
R_{avg}	1.39	1.61	1.42	1.39

Table 14. Extreme values of R_{avg}.

	Svartodden	Camp Morton	Marjaniemi
h_c^D(max) / h_i^T(min)	1.95 / 1.01=1.93*	1.28 / 0.7=1.83	1.03 / 0.5=2.06
h_c^T(max) / h_i^T(min)	1.82 / 1.01=1.80*	1.34 / 0.7=1.91	0.92 / 0.5=1.84
h_c^T(min) / h_i^D	1.61 / 1.16=1.39	1.13 / 0.85=1.42	0.71 / 0.6=1.15

*The (h_i^T - h_i^D) that was found in the Camp Morton ridge is assumed also in 1998

Table 15. The coefficient in Stefan's law, h_c from Eq. (5), the measured values in parenthesis (m).

	η	ω	h_c^T (min), h_i^M	h_c^T (min), h_i^T (min)	h_c^T(max), h_i^T (max)
Svartodden	0.33	0.35	1.67 (1.62)	-	-
Camp Morton	0.35	0.30	1.22 (1.13)	1.10 (1.13)	1.30 (1.34)
Marjaniemi	0.35	0.90	0.80 (0.71)	0.71 (0.71)	0.90 (0.92)

Table 16. The limit value of R_{avg} as a function of l_r in Eq.(6). l_i=0.85l_{pi} and b=1.

l_r	0.10 l_{pi}	0.15 l_{pi}	0.20 l_{pi}	0.25 l_{pi}	0.30 l_{pi}	0.35 l_{pi}
η (%)	16-20	22-27	28-32	33-37	39-42	44-47
R_{avg}	2.92	2.38	2.06	1.84	1.68	1.56

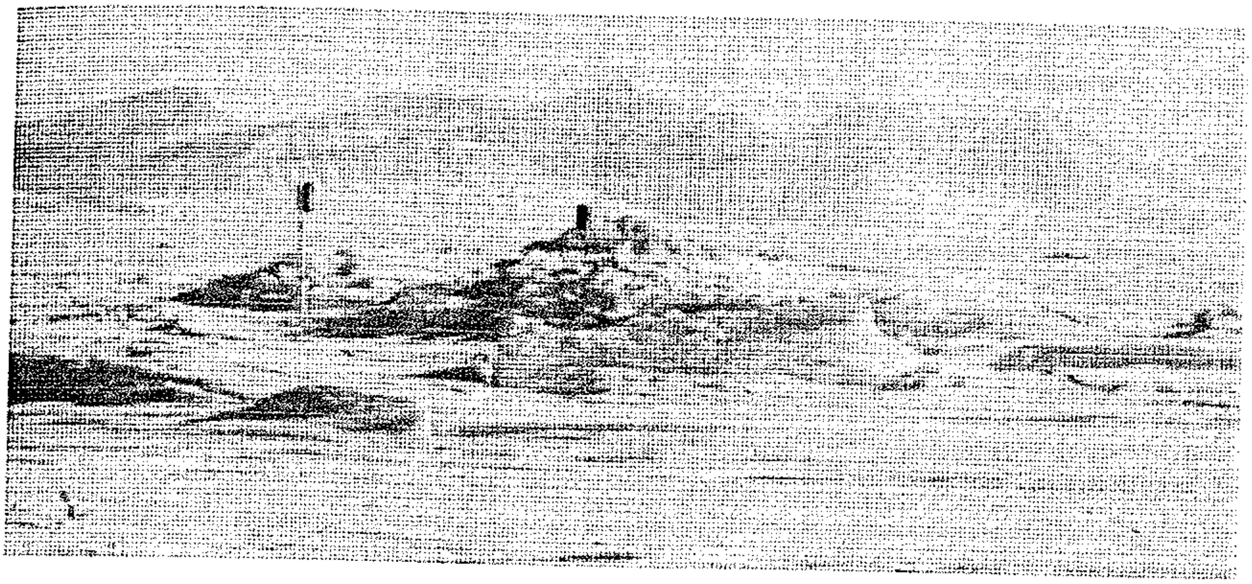

Fig. 1. A ridge in the Van Mijen fjord on Spitsbergen (photo by Bjarne Bergheim).

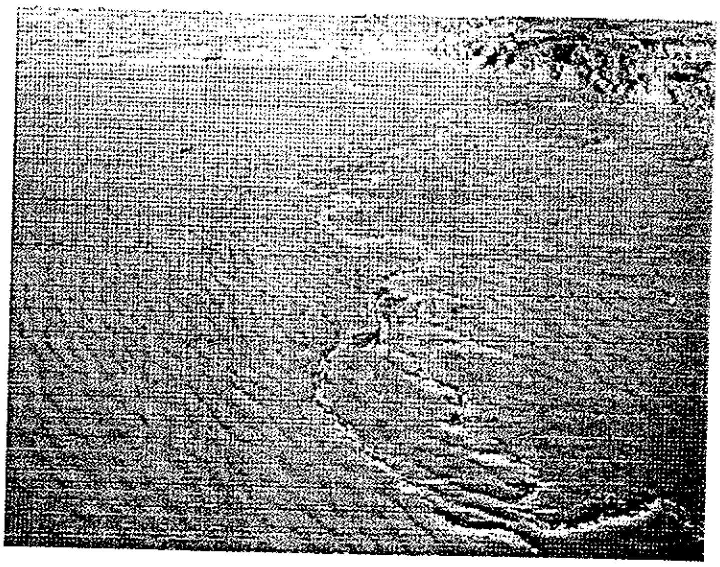

Fig. 2. A ridge in front of the Tuna Glacier in the Tempel fjord on Spitsbergen the winter of 1999 (photo by Stian Soltvedt).

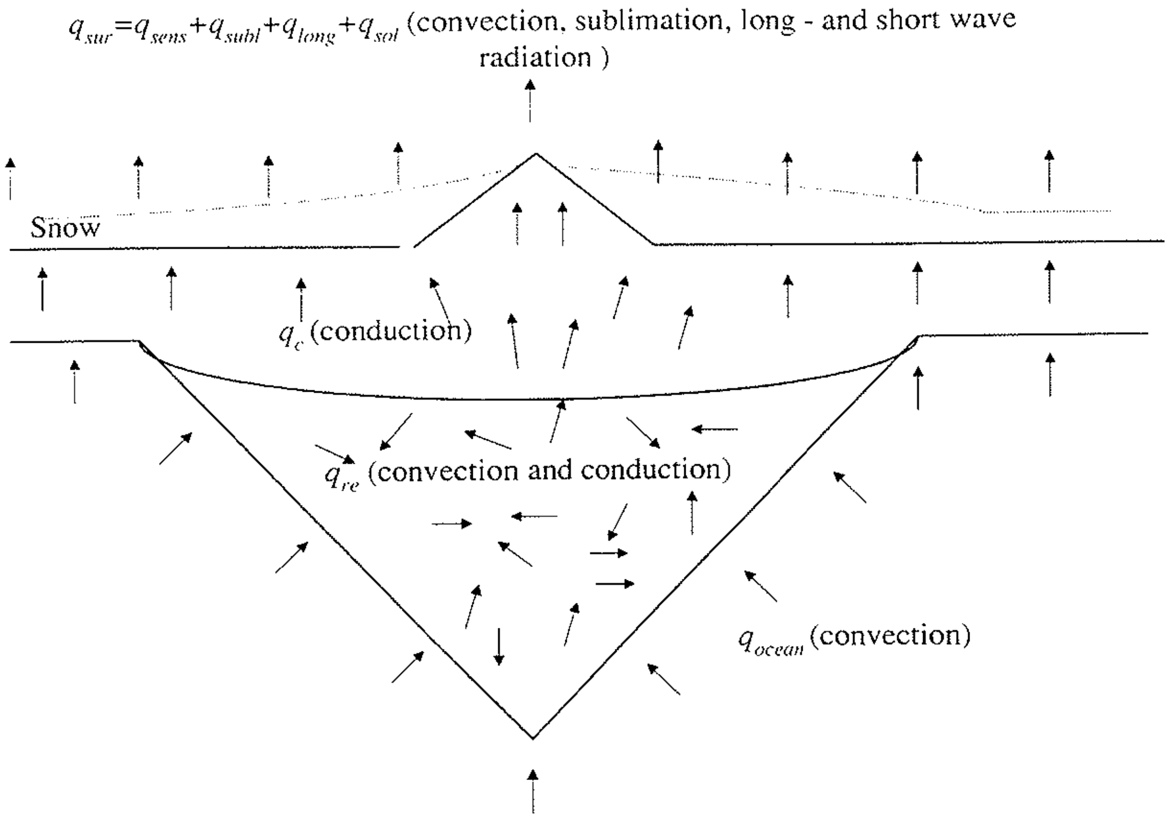

Fig 3. Illustration of the different fluxes and heat transfer mechanisms in an ice ridge.

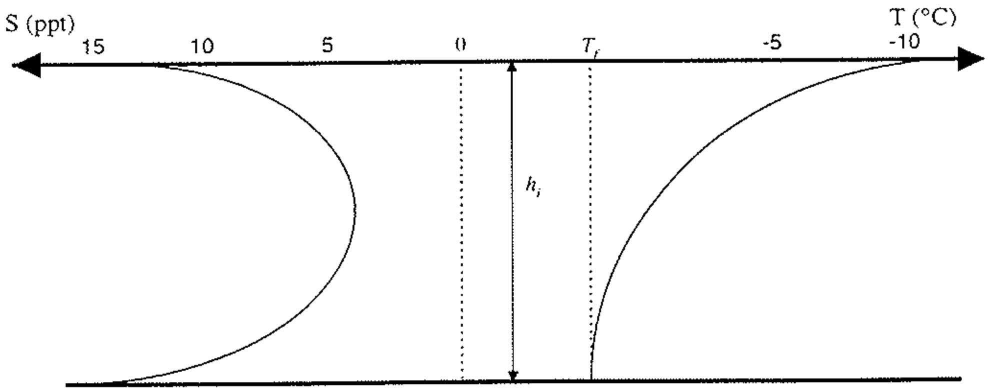

Fig. 4. Typical temperature and salinity profile in young sea ice

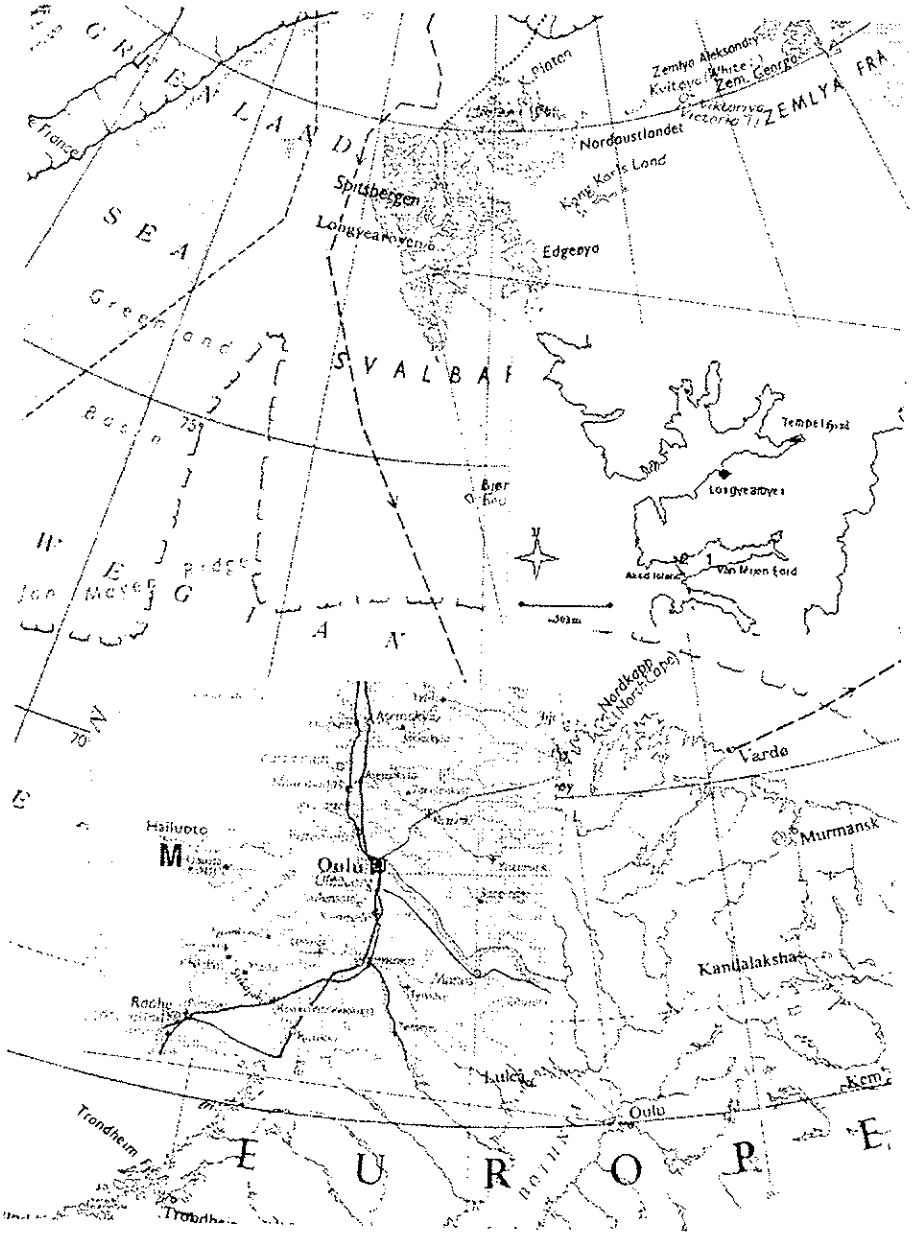

Fig. 5 Map of the sites. The M on the left map indicates the Marjaniemi ridge, and the 1 and 2 indicate the Svartodden and Camp Morton ridges, respectively.

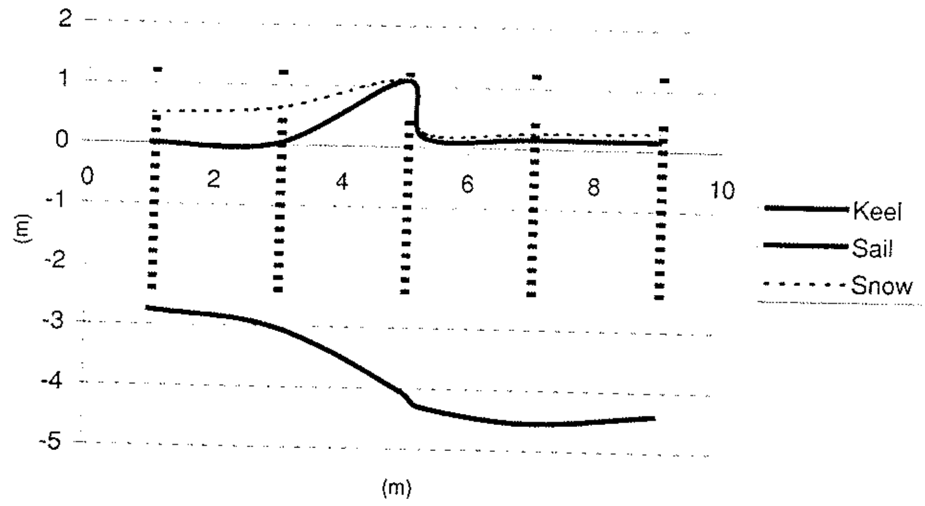

Fig. 6. The thermistor strings in the Camp Morton ridge

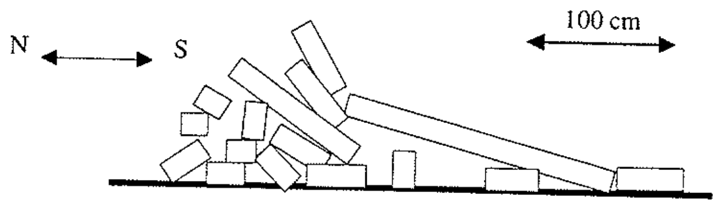

Fig. 7. Sketch of the structure in the sail of the Camp Morton ridge, north to the left.

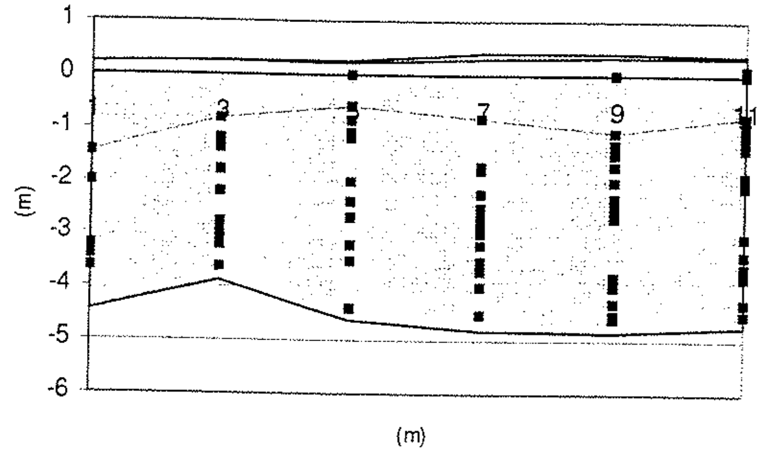

a)

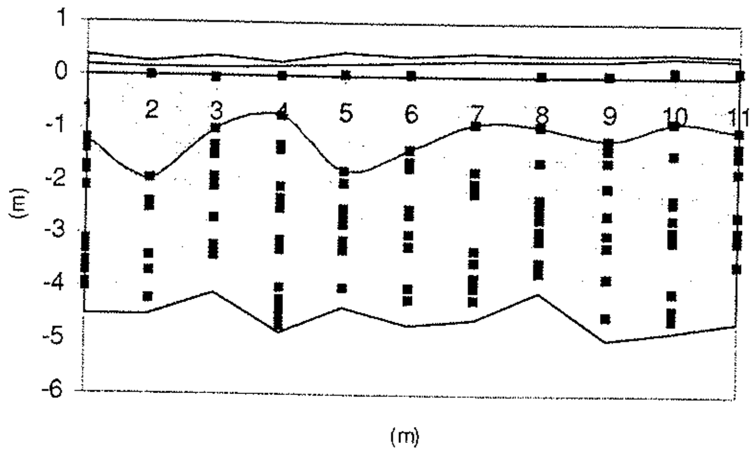

b)

Fig. 8. The thermistor cross section at Marjaniemi. The grey area is the keel, the white the sail, the dotted white the snow and the black dots are pores. a) 26.02.99 b)25.03.99.

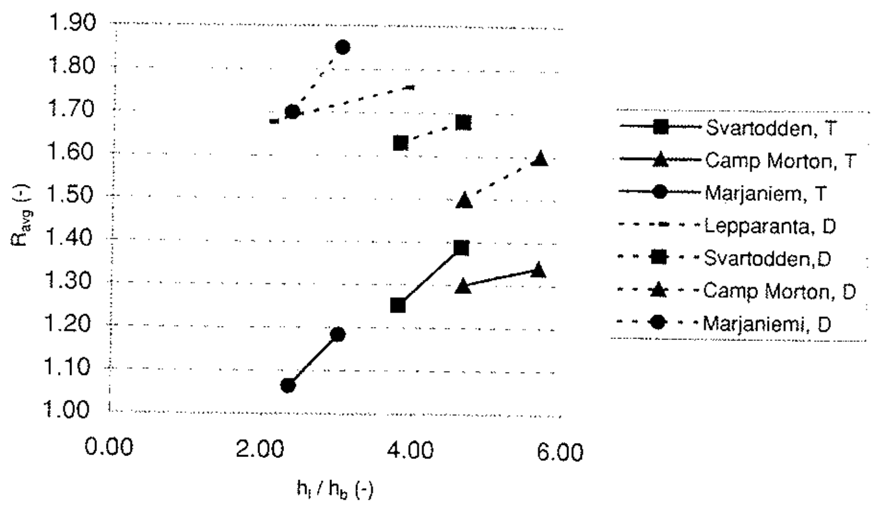

Fig. 9. R_{avg} versus the ratio of the level ice thickness to the block thickness (h_i / h_b). T – temperatures and D – drillings.

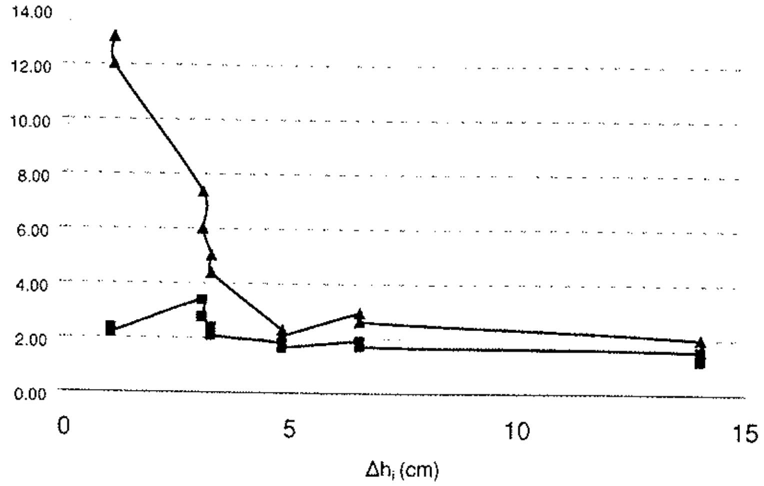

Fig. 10. Timco and Goodrich (1988) laboratory work, the line with triangles is R_{avg}, whereas the line with sqaures is $\Delta h_c / h_i$.

Chapter 3

Measurements of temperature distribution, consolidation and morphology of a first-year sea ice ridge

Journal of Cold Regions Science and Engineering, 29 (1999), pp. 59 – 74.

Chapter 4

Simulations of the consolidation process in first-year sea ice ridges

Submitted to the Journal of Cold Regions Science and Engineering

Chapter 5

LOLEIF ridge experiments at Marjaniemi; the size and the strength of the consolidated layer

Proceedings of the 15th International Symposium on Ice (IAHR), Gdańsk, Poland, 28 August–1 September 2000, Vol. 1, pp. 45-52.

Notation

Symbol:

T	temperature
h	height / thickness
σ	stress
ε	strain

Indices:

c	consolidated layer
i	sea ice
f	freezing point

LOLEIF ridge experiments at Marjaniemi;

the size and strength of the consolidated layer

Knut V. Høyland[1], Guro Kjestveit[1], Jaakko Heinonen[2] and Mauri Määttänen[2]
[1]The Norwegian University of Science and Technology (NTNU), Trondheim, Norway
[2]The Helsinki University of Technology (HUT), Espoo, Finland
knut.hoyland@bygg.ntnu.no

ABSTRACT

Measurements of spatial and temporal temperature development, geometry, porosity, salinity, density, crystal structure and uniaxial compression strength of a first-year ice ridge field have been performed. Thickness, salinity and density of the level ice were also measured. The test site was a large ridged area with 3 - 6 layers of rafted ice, the keel depth ranged from 4 to 9 m and the average porosity of the unconsolidated rubble was 38 %. The strength of the ice had a clear dependency of the depth below the water line from which it was taken: below and above 0.85 m. The strength of the consolidated layer was 5 – 7 MPa. The temperature measurements showed that the consolidated layer ended up being between 0.71 and 0.92 m, the drillings predicted a thicker layer, 1.05 - 1.11 m.

INTRODUCTION

Sea ice ridges are formed by compression or shear in the ice cover. They are usually created by environmental forces such as winds and currents and especially in the shear zone between the landfast and drift ice. Ridges are porous features consisting of ice blocks, slush, water and in the sail also air and snow. The keel is often divided into an upper consolidated layer and a lower part of unconsolidated rubble. The consolidated zone grows throughout the cold seasons. Ridges may represent the design load for ships, coastal and offshore structures in many arctic and sub-arctic marine areas. It is however not clear what load a first-year ridge can exert on a given structure or how the ridge deforms. The loads are usually calculated by assuming that the load contributions from the sail, the consolidated layer and from the keel can be found independently and then added up (see eg Krankkala and Määttänen, 1984). Different ridge failure modes observed at the Molikpaq platform is reported by Timco et al. (1999). For a large number of the ridges the first failure occurred in the level ice behind the ridge. The ridge itself failed in different modes: shear, bending or spine failure. They reported that the measured loads were lower than those given by different load algorithms. Increased knowledge about the internal structure of first-year ridges is necessary to improve these load estimates. Crushing is the worst case scenario for the consolidated layer. Thus its size and compression strength are of special importance. We are in the following concerned with the consolidated zone, its size and the derivation of its material and physical properties. Several researchers (eg Leppäranta et al. 1995; Croasdale et al. 1990; Frederking and Wrigth 1980; Kankaanpää 1997; Timco and Goodrich 1988) have studied the vertical extension of the consolidated layer and it seems to be between 1.3 and 2 times the level ice thickness. It is however, not clear how the consolidated layer should be defined, nor does it seem to exist a standardised method for examining the thickness of this layer. The water line is often used as an upper boundary as the blocks are loosely bound in the sail. The lower boundary is more difficult because it exists a partly consolidated layer beneath the fully refrozen one. This partly consolidated layer is a porous high temperature zone with less mechanical strength than the fully refrozen one, but the strength is probably higher than for the unconsolidated rubble. The determination of the lower boundary can be done either in a thermal-, or in a mechanical sense. If the thermal one is chosen, then the temperature becomes the prime indicator of consolidation. The temperatures in the consolidated layer are said to be below the freezing point. The measurements can be made by coring or by installing thermistor-strings. The thermal definition has the advantage that it is precise and that it is clearly related to measurements. The disadvantage is that it excludes the partly consolidated layer and that it takes more time and money than drilling. A mechanical definition will be related to a pronounced drop in some mechanical strength at a certain depth level. The best way to examine this is to take samples from different depths, and do eg uniaxial compression tests. This is time and money consuming, so another popular way is by drilling. The major advantage of drilling is that it is quick to perform. It is however less precise as it depends to a larger degree on the driller. Another disadvantage is that it is more destructive so it becomes difficult to examine the temporal development.

The thermal definition seems to estimate a thinner consolidated layer than what is found by drilling (Høyland, 2000).

EXPERIMENTAL

The field-work was a part of the LOLEIF project and took place at Marjaniemi scientific station at the island Hailuoto outside Oulu in the north of Finland. The Helsinki University of Technology (HUT) organised and was responsible for the field-work. The work reported in this paper was a co-operation between HUT and the Norwegian University of Science and Technology (NTNU). The test site was located in an 8 km long chain of different shear - and pressure ridges off shore the western coast of Hailuoto. The ice formed in December and stayed until the first half of May. Six thermistor-strings were installed along a line in the rubble, and one in the level ice. Dataloggers were attached to all of the strings and logged the temperatures every sixth hour from 26 February to 25 March. The porosity and geometry was examined by drilling. The thermistor-strings, dataloggers, drilling equipment and procedures are described in Løset et al. (1998). Meteorological conditions were recorded at the scientific station at Marjaniemi. Ice was cut from the consolidated layer to make uniaxial compression tests and to measure salinity and density. The salinity and density measurements were done at location, whereas the horizontal uniaxial compression tests were done at the University of Oulu. The density measurements were performed by mass divided by volume. The volume was measured by putting the samples into a plastic bag, submerging it in water and measuring the displaced volume. One set of the samples was left to drain for between 0.5 and 1 hour before measuring. The other set was taken directly from the water. The salinity, density and thickness of the level ice were also measured. The samples for the compression tests were cylindrical with length from 134.5 to 151.5 (mm), and diameter varying from 67.5 to 69.5 (mm). The tests were performed according to IAHR guidelines; the temperature of the ice was −10°C, the velocity of the pushing plate was constant, ie almost constant strain rate of 10^{-3} s^{-1}. The force and the displacement were recorded, and some of the tests were recorded on video.

RESULTS

Geometry, morphology and porosity

The ridge was probably formed around 20 January 1999. The meteorological data show low pressure, low visibility and high wind-speed around this date. Simulations also show that the level ice thickness was about 0.2 m at that time (Høyland, in prep). It was a large ridge area with 3 - 6 layers of rafted ice. The depth of the keel ranged from 4 to 9 metres, and was about 4.5 metres in the thermistor-area. The depth of the keel seemed to be independent of the visible sail. The thickness of the rafted layers was 0.2 m. The average porosity of the total keel in the thermistor-area was 0.34, whereas it was measured to be 0.38 in the unconsolidated part. A decreasing porosity was found in the three cross-sections that were drilled twice.

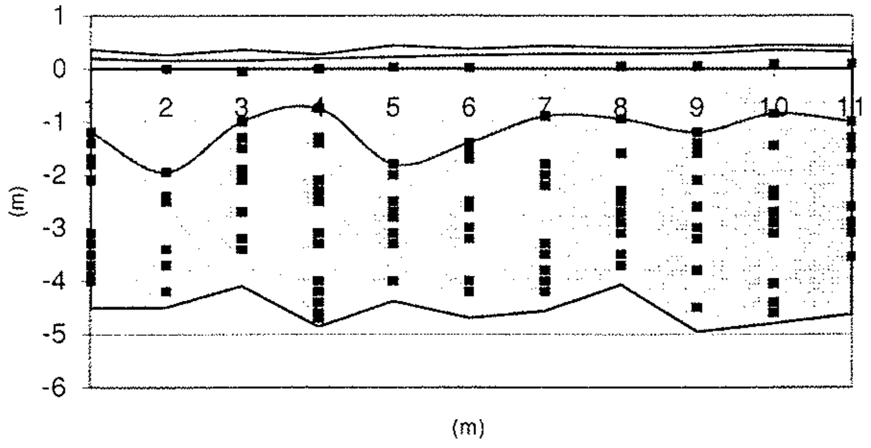

Fig. 1. The thermistor cross-section 25.03.99. The black dots are pores, the grey area is the keel, the white area is the sail and the white dotted area is the snow layer. The solid lines represent the consolidated layer as being found by drillings

Salinity and density

Samples were taken from the consolidated layer and the level ice to measure salinity and density 23 and 24 March 1999. The results are displayed in Fig. 2.

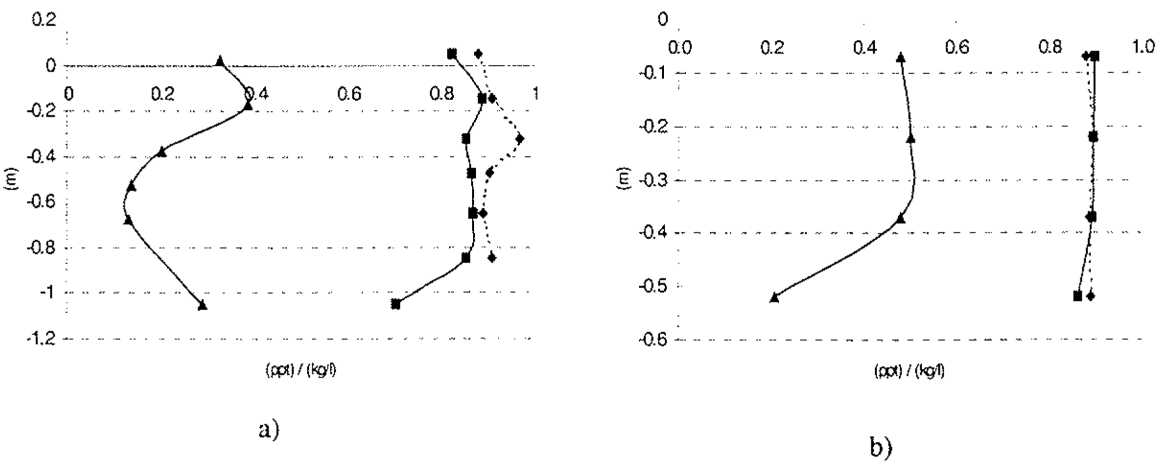

Fig. 2. Vertical profile of salinity and density measurements. The solid line with triangles represents the salinity (ppt), the solid line with squares represents the drained density (kg/l) and the dotted line the undrained density (kg/l); a) the ridge and b) the level ice.

The standard deviation for density measurements of the consolidated layer was 0.03 (kg/l) for the undrained - and 0.06 (kg/l) for the drained samples. The corresponding values were 0.01 (kg/l) and 0.02 (kg/l) for the level ice.

Consolidation, level ice thickness and meteorological conditions

Thermistor-strings through an ice sheet can be used to measure its thickness. Table 1 displays the measured thickness of the level ice and the consolidated layer. It was a normal winter at Hailuoto; the cumulative freezing degree-days (*FDD*) for the growth period was 138°C days.

Table 1. The thickness of the level ice and the consolidated layer (m).

	Level ice thickness, h_i		Consolidated layer thickness, h_c	
Date	26.02.99	25.03.99	26.02.99	25.03.99
Drilling	0.47	0.60	0.87*	1.11*
Temperatures	0.4 – 0.5	0.5 – 0.6	0.5 – 0.71	0.71 – 0.92

*Average values from the neighbouring cross-sections gave 0.83 and 1.05.

Compression tests

The results from the compression tests are summarised in Fig. 4 and Table 2.

Table 2. Results from the compression tests, average values and standard deviation.

Depth (cm)	Number of tests	Av. strain at Max. Comp. Stress - $\overline{\varepsilon}$	Av. max. comp. stress $\overline{\sigma}_{max}$ (MPa)	Av. stress at $\overline{\varepsilon}$=0.06 $\overline{\sigma}_{0.06}$ (MPa)
15 to –5	6	0.017 ± 0.004	5.0 ± 1.9	1.9 ± 0.9
-5 to –25	12	0.016 ± 0.006	5.2 ± 1.8	2.1 ± 0.7
-25 to –45	10	0.017 ± 0.005	7.2 ± 1.6	2.4 ± 0.7
-45 to –65	7	0.017 ± 0.006	6.2 ± 1.1	2.5 ± 0.5
-65 to –85	4	0.016 ± 0.003	4.8 ± 0.9	2.4 ± 0.2
-85 to –105	3	0.044 ± 0.020	1.5 ± 0.4	1.3 ± 0.6
-105 to –125	4	0.039 ± 0.024	1.7 ± 0.6	1.2 ± 0.7

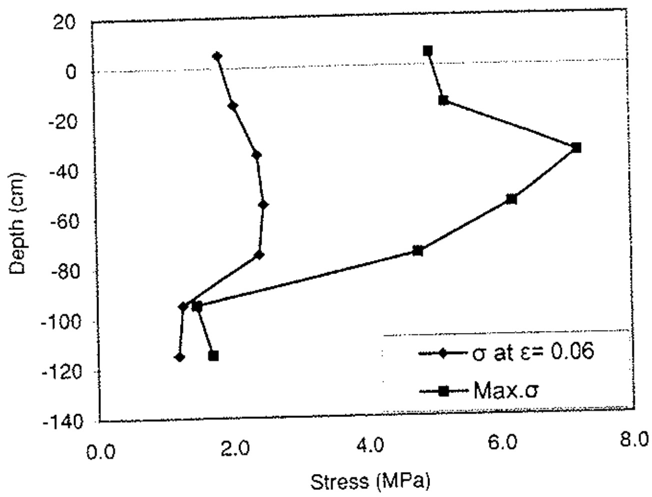

Fig. 4. The average maximum stress (σ_{max}) and the average stress at strain equal to 0.06 ($\sigma_{0.06}$) versus depth.

The samples from the consolidated zone can be divided into two groups: samples without initial failures (undamaged ice), and those with initial failures (damaged ice). All the undamaged samples had similar stress-strain curves, an example is shown in Fig. 5 a). The damaged ice did not have a typical pattern, and σ_{max} was less than for the transparent ice as shown in Fig. 5b). No significant difference could be found for $\sigma_{0.06}$ (the average stress at $\varepsilon = 0.06$) regardless of stress history or initial damage. It should also be noted that the average strain at peak stress was about the same for depths above –0.85 m.

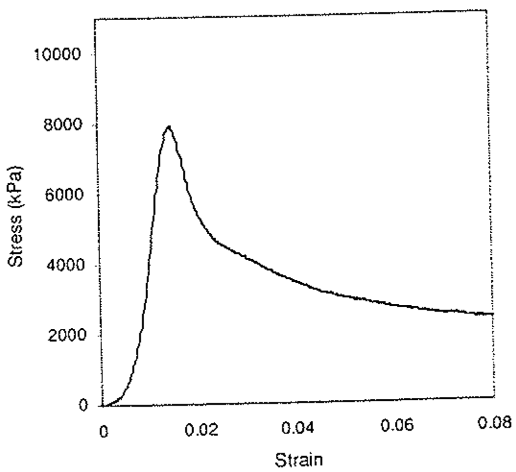

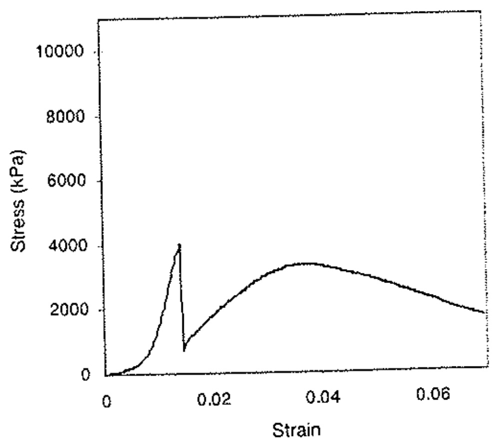

Fig. 5. Stress-strain curves: a) An initially undamaged sample and b) An initially damaged sample.

DISCUSSION

Physical and mechanical properties

The salinity and density measurements are comparable to what has been found by others (Kankaanpää, 1997, Leppäranta et al., 1995 and Veitch et al., 1991). The strength of the different depths seems to be related to the salinity and the density. The two highest compression strengths were found between 0.25 and 0.65 below the water-line, and this is where the two lowest salinity values were measured. The peak strength also corresponds with the maximum density. Though the numbers of samples were limited some comparison between the consolidated layer and the level ice can be done. The density measurements show a bigger scatter for the consolidated layer than for the level ice, this is an indication that such a scatter may also yield for mechanical properties. This means that even if similar average values for some mechanical property of level ice and consolidated zone is measured, the strength of the total consolidated layer may still be less due to the weak points. Any use of tests such as these to predict real behaviour is faced with complicating factors such as scaling and the temperature dependence of ice strength. Table 3 presents some other results of compression tests of samples from the consolidated zone. Our values are a bit higher, but still comparable. An increasing strength with depth is also found by Veitch et al. (1991).

Table 3. Compression test of the consolidated layer in ice ridges (MPa).

Testing temp.	Veitch et al., Lab. closed loop, horizontal, $\dot{\varepsilon} = 2 \cdot 10^{-3}$		Frederking and Wright, in field, vertical, $\dot{\varepsilon} = 10^{-5} - 4 \cdot 10^{-4}$
	depth (m) = 0 – 0.2	depth (m) = 0.2 – 0.4	-
T=-8°C	3.8 ± 1.2	5.2 ± 1.4	-
T=-20°C	6.2	6.8 ± 2.6	-
T=-19°C	-	-	2.3 – 13.3

The thickness of the consolidated layer

The pronounced drop in mechanical strength of the samples taken from below 0.85 m is reasonable to interpret as a mechanical definition of the consolidated layer. But note that the compression test were done at −10°C, and that the in-situ temperature in the lower parts are close to T_f. Thus an artificial high strength may have been measured. The values in Table 4 show that the thickness of the consolidated layer predicted by the uniaxial compression tests and the temperature measurements correspond well, and that the drillings predict a thicker layer. These data suggest that a thermal and a mechanical definition of the vertical extension of the consolidated layer correspond fairly well, and that the drillings include a partly consolidated layer and thereby overestimates the thickness of the consolidated zone. The growth of the consolidated layer during the measured period did not seem to be affected by the method of investigation.

However any choice of definition or method of investigation should always be closely related to the purpose of the investigation.

Table 4. The final thickness of the consolidated layer by the different methods (m).

	Temperatures	Compression tests	Drillings
h_c	0.71 – 0.92	0.85	1.05 - 1.11

CONCLUSIONS

Measurements of spatial and temporal temperature development, physical and mechanical properties of a first-year ice ridge field have been done. Level ice conditions were also measured. The major findings are:

- The average uniaxial compression strength of the consolidated layer was 5 – 7 MPa
- The average strength of the partly consolidated layer was 1.5 – 1.7 MPa
- The porosity of the unconsolidated part of the keel was 38 %
- The final thickness of the consolidated layer was investigated in three ways:

  -Temperature measurements: 0.71 – 0.92 m

  -Compression tests: 0.85 m

  -Drillings: 1.05 – 1.11 m
- The growth of the consolidated zone did not seem to be affected by the method of examination

Acknowledgement

This work has been undertaken within the LOLEIF-project in the framework of the EU-sponsored Marine Science and Technology (MAST-III). Programmed under contract no.MAS3-CT97-0078. Seppo Meriläinen, Olli Kamunen and Kai Riihinen, the technicians from HUT, were indispensable. In addition were Denis Tazov from Mockba, Jeff Weaver from Exxon, and many students from the University of Oulu assisting in the fieldwork. The University of Oulu performed the compression test. We would also like to thank DNV, UNIS and the Norwegian Research Council for financial support.

References

Croasdale, K.R., Allen, N.F.B. and Marcellus, R.W. 1990. Thermal response of ice rubble: predictions and observations. Proceedings of the 10th International Symposium on Ice (IAHR), Espoo, Finland 20-24 Aug. 1990, Vol. 1, pp. 153-167.

Frederking, R.M.W. and Wright, B. 1982. Characteristics and stability of an ice-rubble field Issungnak, February-March 1980. NRC Technical memorandum, Jan 1982, No. 134, pp. 230-247.

Høyland, K.V. Simulations of the consolidation process in first-year ice ridges, in prep.

Høyland, K.V. 2000. Measurements of consolidation in three first-year ridges. Proceedings of the 15th International Symposium on Ice (IAHR), Gdańsk, Poland, 28 August - 1 September, Vol. 1, pp. 19-26.

Kankaanpää, P. 1997. Distribution, morphology and structure of sea ice pressure ridges in the Baltic Sea. Fennia 175:2, pp 139-240. Helsinki, ISSN 0015-0010.

Krankkala, T. and Määttänen, M. 1984. Methods for determining ice forces due to first- and multi-year ridges. Proceedings of the 7th International Symposium on Ice (IAHR), Hamburg, Germany 27-31 Aug. 1984, Vol. 4, pp. 263-287.

Leppäranta, M., Lensu, M., Kosloff, P. and Veitch, B., 1995. The life story of a first-year sea ice ridge. Cold Regions Science and Technology 23 (1995), pp. 279-290.

Løset, S., Langeland, A., Bergheim B. and Høyland, K.V., 1998. Geometry and physical properties of a stamucha found on Spitsbergen. Proceedings of the 14th International Symposium on Ice (IAHR), Potsdam, New York, USA, 27-31 July 1998, Vol. 1, pp. 339-344.

Timco, G.W., Wright, B., Johnston, M. and Frederking, R. 1999. First-year ice ridge loads on Molikpaq. Proceedings from Russian Conference on Arctic Offshore Engineering (RAO), St.Petersburg, Russia, 6-9 July 1999, Vol. 2, pp. 172-179.

Timco, G.W. and Goodrich, L.E. 1988. Ice rubble consolidation. Proceedings of the 9th International Symposium on Ice, Sapporo, Japan, 1988, pp. 426-438.

Veitch, B., Lensu, M., Riska, K., Kosloff, P., Keiley. P. and Kujala, P. 1991a. Field observations of ridges in the northern Baltic Sea. Proceedings of the 11th International Conference on Port and Ocean Engineering under Arctic Conditions, St. John's, Canada, pp. 381-400.

Chapter 6

Monitoring and observation of the formation of a first-year ice ridge field

Proceedings of the 15th International Conference on Port and Ocean Engineering under Arctic Conditions (POAC), Espoo, Finland 23-27 August 1999, Vol. 1, pp. 37-48.

Notation

Symbol:

N	force per metre
ρ	density
g	acceleration due to gravity
λ_0	half wave-length
σ	stress
w	vertical deflection
h	ice thickness
I	second moment of inertia
T	temperature

Indices:

w	seawater

MONITORING AND OBSERVATION OF THE FORMATION OF A FIRST-YEAR ICE RIDGE-FIELD

Knut V. Høyland and Sveinung Løset
Department of Structural Engineering,
Norwegian University of Science and Technology, Trondheim, Norway &
The University Courses on Svalbard, Norway

ABSTRACT

The development of a ridge-field in the Tempel fjord on Spitsbergen was observed during the late winter 1998. The ice was stressed by a moving glacier, and this probably caused the ridging. The speed of the glacier was estimated to 0.2 m/day. The ridge-field was parallel to the glacier front and about 3 km long. Several almost parallel ridges developed in the central parts. The ridge-field porosity measurements ranged from 6 to 30 %. A maximum keel depth of 6 m was detected. The salinity measurements showed big variation and indicate substantial brine drainage. The thickness of pieces in the sail varied from 0.2 m and up to the parent ice thickness from which it was formed (up to one metre). The level ice grew from 0.85 m to 1.2 m. It buckled and failed in bending, but horizontal splitting or shearing of the floes seems to have occurred. It also seems as if the crushing was minor during the ridge formation. Possible mechanisms for the deformation/fracture of the ice are discussed.

1. INTRODUCTION

Sea ice ridges are formed by shear or compression in the ice cover, often by the closing of an open or refrozen lead. Physical environmental forces such as wind and/or currents are often the driving forces. This phenomenon is a complicated process, and has been studied by several researchers, for instance Parmerter and Coon (1972 and 1973) and more recently by Hopkins and Tukhuri (1998) and Tukhuri et al. (1998). A failure in the ice cover does not necessarily lead to ridging, rafting is another important process. Tukhuri and Hopkins have studied this both in laboratory and numerically and they claim that the thickness distribution of the ice sheet is the key feature. A uniform ice sheet will raft whereas non-uniform sheets will ridge. The fracture pattern of the ice cover in a ridging process is not clear. Obviously the floes will often fail in bending, but horizontal splitting may also be involved. Non-uniform material properties and vertical temperature gradient through the ice can create a complicated stress pattern.

If an ice sheet is stressed and the loading rate is low, then the sheet may deform in creep buckling. As the deformation increases, the stresses in the bottom and on the top of the waves will increase. When a critical level of stress, strain rate or strain is reached, fracture is initiated and a ridging process may start.

During the late winter 1998 we monitored the formation of such a ridge-field. The movement of the Tuna glacier probably provoked the event. The ice creep buckled prior to fracturing and ridging.

2. THE SITE AND PERFORMANCE OF WORK

The ridge-field was located in the Tempel fjord on Spitsbergen at approximately 78º26'37'' north and 17º22'36'' east (see Figure 1). The Tempel fjord is long and narrow and the ice conditions are stable throughout the winter. The two polythermal glaciers Tuna and Van Post both terminate in the far end of the fjord. Fresh water leakage occurred and created some stratification in the fjord during experiments performed in 1994 (Tverberg, 1994), and there is no reason to believe that this has stopped. The Tuna glacier moved during the winter of 1998, this could have been a mini-surge. The movement stressed the ice and we believe that this was the basic reason for the creation of the ridge-field. During the last years (1996-1997) no such ridge-field was observed. The movement of the glacier was probably not affected by the presence of sea ice, so that the ridging was deformation controlled.

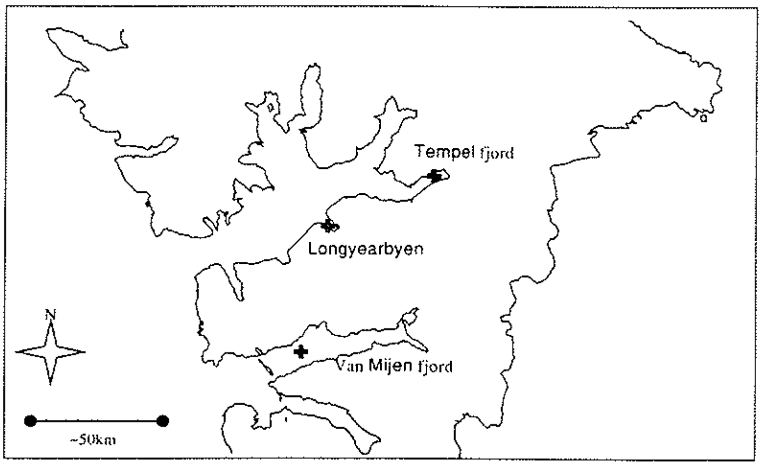

Figure 1. Map of the area.

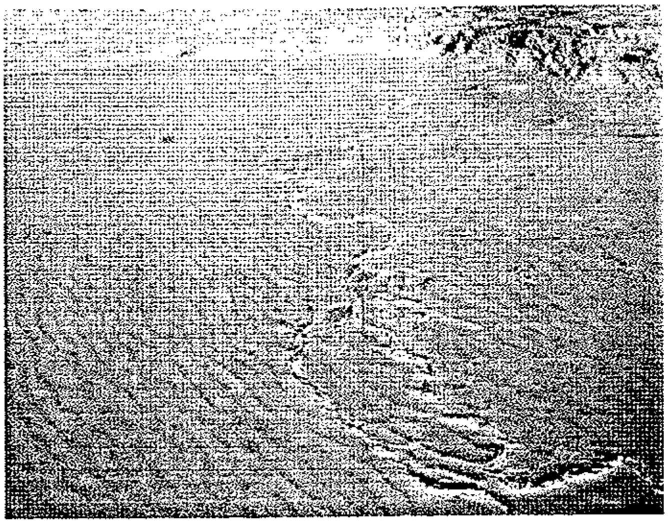

Figure 2. Air photography of the northern half of the ridge 30.03.98. The glacier is on the top of, and to the right (east) in the picture (Photo by Stian Soltvedt).

The ridge-field was roughly 3 km long, situated at a water depth of about 45 m, approximately 400 m from the front (west) of the Tuna glacier. 19 February there was only one ridge, but during the season up to four parallel ridges appeared. Figure 2 shows a picture of the northern half of the ridge where we can see that two parallel ridges have developed. Most of the ridging occurred in the centre of the fjord (in the middle of the ridge-field).

The site was visited 6 times of which the first, 19 February, was survey. Table 1 displays the workplan. A new ridge developed at one of our visits, between 11 and 12 March (see Figure 3). The development of the keel geometry and the porosity was determined by drilling holes through two different cross sections. The drilling equipment and procedures are described in Løset et al. (1998). Cores were taken from the ridge to determine salinity. A theodolite was used in the levelling of the surface, and to measure the relative movement of the glacier to several points on the level ice.

Table 1. Workplan for the visits at the ridge-field. C.S. = Cross-section.

	Date				
	11-12.03.98	26.03.98	02.04.98	21.04.98	05.05.98
Drilling	C.S.1/C.S.2	-	-	C.S.2	C.S.1/C.S.2
Surface elevation	C.S.1/C.S.2	C.S.1/C.S.2	-	C.S.1/C.S.2	C.S.1/C.S.2
Horizontal contraction		C.S.1	C.S.1	C.S.1	C.S.1
Salinity samples				C.S.2	

a)

b)

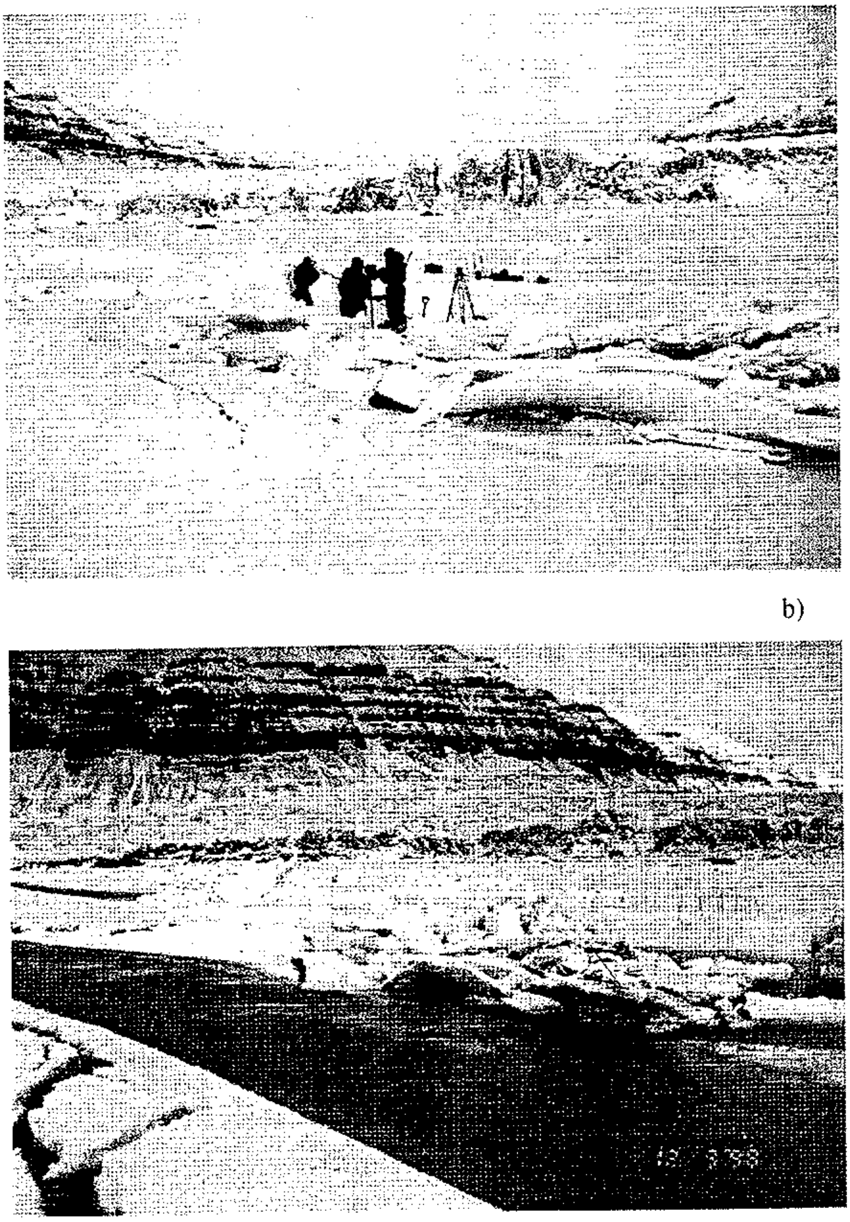

Figure 3. Cross section 1 at a)11 March and b)12 March

3. RESULTS and discussion

3.1 Geometry and morphology

Figure 2 shows the northern half of the ridge 30 March. From this photo we can see that the ridges followed a curvilinear shape. It was about 3 km long. Only one ridge had formed at our first visit (19 February), whereas at our last visit (5 May) up to four parallel ridges had formed along the central parts of the ridge-field. Table 2 shows the number of visible ridges in the two cross sections at our different visits.

The surface was highly irregular (see Figure 4). The typical idealisation of a ridge as a linear and symmetrical figure consisting of a triangular sail and keel was not observed. The ridge can however be considered as piecewise linear and characterised by cross-sections. Sail heights of up to 1 m, and keel depths down to 6 m were typical.

Table 2. Number of visible ridges in the two cross sections at different dates.

	Date				
	19.02.98	12.03.98	26.03.98	21.04.98	05.05.98
C.S. 1	1	2	2	2	3
C.S. 2	1	2	3	3	4

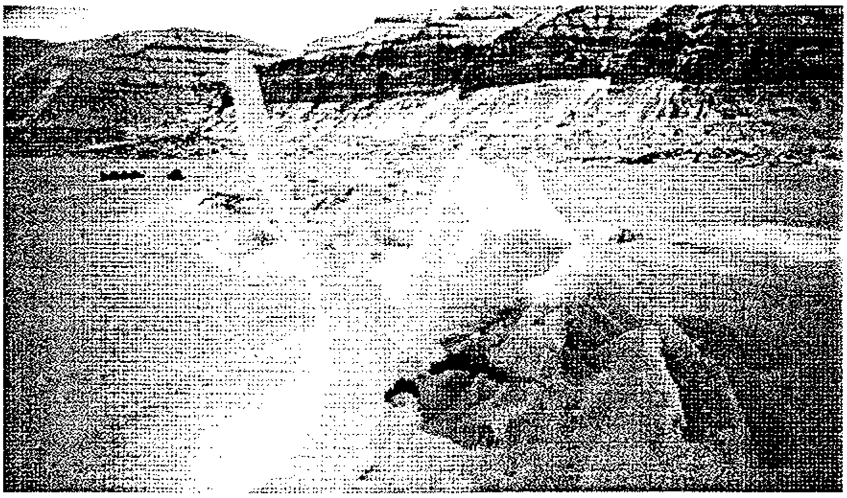

Figure 4. The surface of the ridge-field.

Figure 5 shows cross section 2 at two different dates. The dotted lines are the surface of the snow and the black parts are pores detected during the drillings. A ridging event happened and a new ridge developed between the two dates. The figure also shows that the keels basically were situated between the visible sails. It also looks like some of the pores that were detected 12 March had refrozen by 21 April. Little deformation of the 'old part' can be seen. The transition between the keel and the water beneath was quite distinct, little slush and crushed ice seemed to be present.

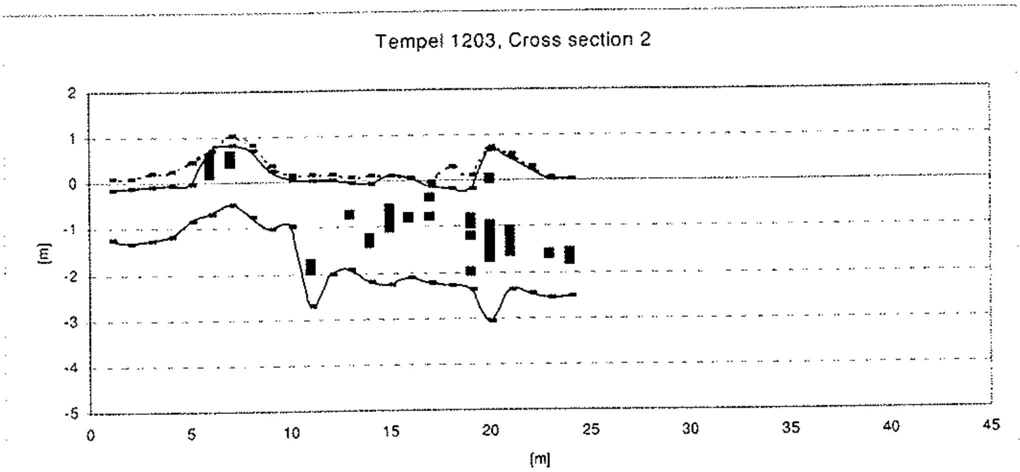

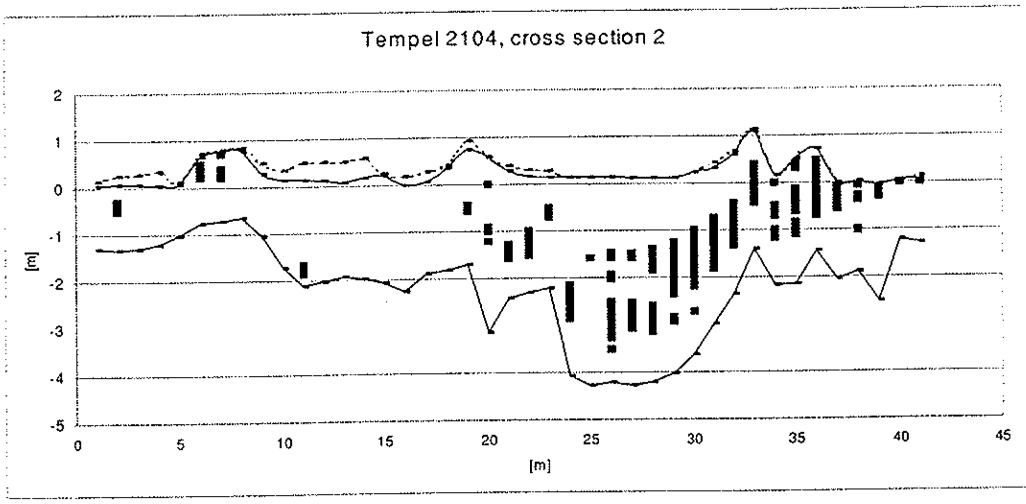

Figure 5. Cross-section of the ridge-field. The dashed line shows the snow surface and the black lines are pores. a) 12.03.98 and b) 21.04.98.

The blocks had different sizes and shapes, but little crushed ice could be seen. The block thickness ranged from 0.2 – 0.3 m and up to level ice thickness at the time of formation. The blocks/floes were often 2-3 metres in the two other directions, in one extreme case a floe of about 5 m × 5 m was standing up. In the youngest ridges standing floes one meter thick were observed. In these thick floes layer like structures could be observed, this was probably due to stratification. Some kind of horizontal splitting or shearing had most likely created these thin blocks.

3.2 Surface elevation, buckling and thickness of level ice

The evolution of the surface in Cross-Section 2 is shown in Figure 6. At least four different ridging events (one prior to 11 March) occurred during the winter. Cross-Section 2 was around 40 m long, and as Table 2 and Figures 5 and 6 show did four almost parallel ridges develop here. In this cross-section were the new ridges formed outside (west of) the old one(s), and did basically not deform the old ridge(s). In the first cross section was most of the ice put into the second ridge, where a floe of 5 m x 5 m was, for a while, standing up. The keel and partly the surface of the old ridge(s) were changed after each ridging event in this cross section. This difference in the two sections is probably due to differences in ridge dynamics.

The distance between points along a line through Cross-Section 1 was measured at four different dates. The distance between the front of the glacier and a point on the level ice west of the ridged area decreased by 9.16 m between 21 April and 5 May. The measurements also showed that the deformation of the ice cover was localised in front (west of) of the ridge-field. The ice cover inside the ridge area (right-hand side in Figure 2) deformed very little, whereas the ice cover outside deformed by creep buckling prior to ridging. Gradually damped waves were observed at least 1 km in front (west) of the ridge-field (Figure 2). The measured contraction of 9.16 m gives a speed of 0.23 m/day, this can be reasonable speed for the movement of the glacier. It does however not seem to be enough to account for the volume of ice in the new ridges that were formed. But we would like to remind the reader that this phenomenon was two-dimensional and our measurements were done only along one line (1-D). This may have caused what seems to be a contradiction.

The level ice thickness increased during the winter. Table 3 shows the measurements at four different dates. The level ice grew quicker than in the Van Mijen fjord, 0.35 m compared to 0.21 m (Kjestveit 1998). A thinner snow cover in the Tempel fjord can explain this difference.

Table 3. Level ice thickness and freeboard (m).

	Date 1998			
	11.03.98	26.03.98	21.04.98	05.05.98
Thickness (m)	0.85	1.09	1.20	1.20
Freeboard (m)	0.05	0.04	0.17	0.10

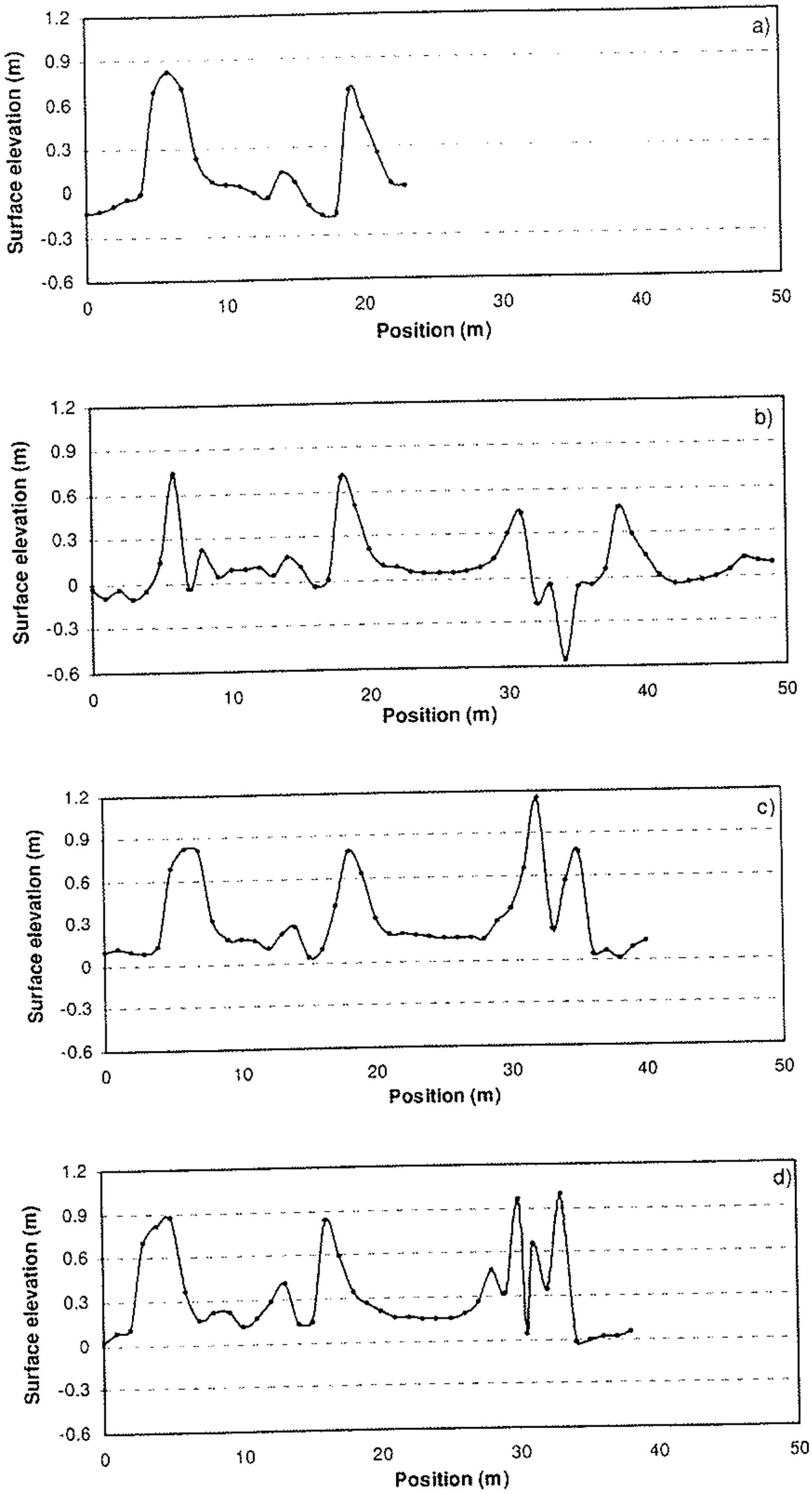

Figure 6. Surface evolution in cross-section 2. a) 11.03.98, b) 26.03.98, c) 21.04.98 and d) 05.05.98.

3.3 Salinity measurements

Table 4 shows the salinity measurements. All the samples were taken 21 April. The two first holes (1 and 14) were in a part of the ridge that was formed before 12 March, the two others after (Figure 5). Hole 41 was drilled through the buckled level ice just outside the ridged area, whereas hole 27 was drilled through the deepest part of the keel. We could however only get samples from the upper parts of the keel in this hole. The high salinity of the water pocket in hole 27 indicates that the water pockets in the keel did not communicate freely with the surrounding seawater. The high salinity in the younger part of the ridge-field (hole 27) compared to the old one (hole 14) indicates that substantial brine drainage occurs. The salinity in the ridge was higher than what was measured in the Van Mijen fjord the same winter (Kjestveit 1998). Less snow made the ice colder, and may have delayed brine drainage. It is also possible that the ridges were formed in different ways and that this could have affected the internal structure and the brine content.

Table 4. The salinity measurements in cross section 2 taken 21.04.98

Holes							
1		14		27		41	
Depth (cm)	Salinity (ppt)	Depth (cm)	Salinity (ppt)	Depth (cm)	Salinity (ppt)	Depth (cm)	Salinity (ppt)
0-3	11	0-3	5	0-3	14	0-3	9
30-33	12	60-63	6	30-33	29	35-38	4
70-73	7	90-93	7	40-43	24	68-71	5
97-100	8	120-123	4	60-63	14	102-105	4.5
130-138	5	150-153	4	75-78	9	125-128	10
Sea water	32	180-183	4	Pore	88	Sea water	35.5
		210-213	4				
		218-221	4				
		223-226	4				
		228-231	6.5				
		Sea water	34				

3.4 Porosity

The measured porosity is shown in Table 5, the column *All* includes all holes that were drilled that day, *Selected* excludes those without porosity, *Old* includes the parts of the ridge that was drilled the previous time and *New* includes the new parts of the ridge. In Cross-Section 2 we can see that the porosity of Holes

1-24 did not change between 12 March and 21 April. This, together with Figure 5, shows that this part did not change. Due to limited time and the fact that the surface of this part had not changed, these holes were not drilled again 5 May. The measured increase in porosity in Holes 24-39 between 21 April and 5 May is probably due to a ridging event, but it can also result from inaccuracy in the measurements. The porosity of the old part increased from 6 to 42 % in Cross-Section 1. This means that ridging had occurred and changed also the old part. Any increase in porosity is of course due to ridging. The porosity of the newly formed parts of the ridges is comparable to what other researchers have found (Leppäranta et al., 1995).

Table 5. Porosity measurements of different selections of the two cross-sections at different dates (units in %).

Cross-Section 1	Date				
	11.03.98		05.05.98		
	All holes	Selected holes	All holes	Selected	Old
No. of holes	25 holes	5 holes	29 holes	24 holes	13 holes
Porosity	6	11	29	30	42

Cross-Section 2	Date					
	12.03.98	21.04.98			05.05.98	
	All	All	Old	New	All	Old
Hole no.	1-24	1-41	1-24	25-39	21-43	25-39
Porosity	11	18	10	25	27	30

4. POSSIBLE SEQUENCE OF FORMATION

The following sequence can explain the ridging events (see Figure 7):

- The glacier moved and stressed the ice-cover.
- The ice sheet buckled (creep buckling). As the wavelength decreased, the stresses and thereby the strain rates (assumption of viscous behaviour) increased.
- A critical level of stress, and/or strain rate (strain) was reached and fracture developed in the trough and on the crest of the wave.
- Water penetrated into the trough of the wave, and ice was piled up on the crest. A new ridge was created, the stresses in the level ice relaxed and the ridging event ended.
- Consolidation of the newly formed ridge and slowly build-up of stresses in the parent ice.

- Buckling etc.

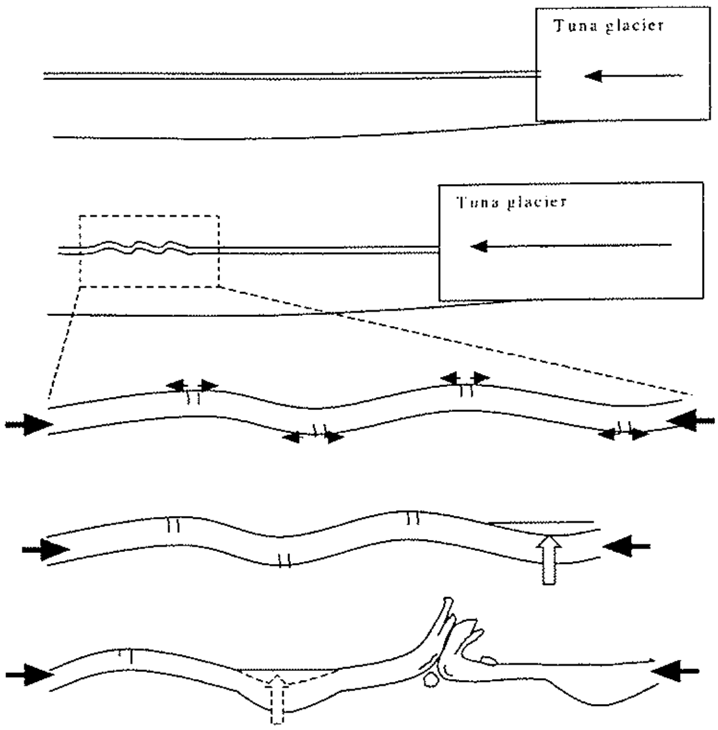

Figure 7. Sketch that shows the possible sequence of formation (vertical cross-section normal to the ridge-field).

Sanderson (1988) has suggested a similar model. The ice fails in bending, and in this way does it not distinguish itself from the classical model of Parmerter and Coon (1973 and 1972). The formation of the keel can though have been different in our case than in 'normal' sea ice ridging. In Figure 7 is it suggested that the keel basically is formed not by blocks being pushed down, but by water flowing in through the crack in the trough of the wave. The position of the pores in Figure 5 b) supports this point. The suggested sequence explains the non-symmetrical keel and sail, the position of the voids in the keel, the irregular surface, and the sharp transition between the keel and the surrounding seawater.

5. CREEP BUCKLING OF AN ICE SHEET

Sanderson (1988) claims that creep strain exceeds elastic strain in ice after a very short time (some seconds). This means that viscous strain probably dominates, and that we have observed creep buckling of an ice sheet. If Calladines analysis (Sandersons, 1988) of creep buckling of a beam is used, then the following relationship between the force per metre (N) and the half wave length (λ_0) can be derived:

$$N = 2\rho_w g \cdot (\frac{\lambda_0}{\pi})^2 \quad (1)$$

where ρ_w is the density of seawater and g the acceleration due to gravity. The maximum stress can be expressed as:

$$\sigma = \frac{w \cdot h \cdot N}{2 \cdot I} = \frac{6 \cdot w \cdot N}{h^2} \quad (2)$$

where I is the second moment of inertia, w is the deflection (vertical), and h is the ice thickness.

On 11 March we measured an ice thickness of 0.85 m, λ_0 to be about 10 m, and the maximum deflection to be 0.53 m. This gives a force N = 204 kN/m, and a maximum stress σ =0.90 MPa. At this point cracks already existed at the crest of the wave, therefore standard beam theory could no longer be applied. The flexural strength of ice at T = -10ºC and a salinity of 5 ppt is about 0.5 MPa (Mellor, 1983). This supports our observations that fracture initiated for a smaller vertical deflection. Eq. (1) shows that the force depends on the half wavelength; for λ_0= 9 m the force becomes N = 165 N/m, and for λ_0= 11 m, N = 247 N/m. λ_0 = 10 m was measured in cross-section 1 in the wave closest to the ridge. Other measurements of wavelengths were not done.

This analysis is simple, material properties and the geometry are simplified. But it does look like some reasonable results can be predicted. Sjølind (1984) has done numerical simulations on creep buckling of ice. He claims that it can be difficult to find the deformation mode that gives critical buckling time.

6. MECHANISMS OF DEFORMATION

The ice sheet was deformed in bending, and fracture was initiated at the top of and in the bottom of the wave. The existence of thin (0.2 –0.3 m) blocks/floes in ridges formed from thick (1 m) level ice shows that some kind of horizontal splitting or shearing probably was involved in the ridging. This does not mean that horizontal splitting occurred before the initiation of the ridging and was a trigger mechanism for it. The thin floes could have been more of a result of the ridging than a cause to it. They could also have been formed from a refrozen layer on the 'river' that was formed in the bottom of the wave (see Figure 7) in the previous ridging, but we do not believe so.

The stress pattern in an ice sheet that is being compressed is complicated. The vertical temperature gradient in the sheet, and the non-uniform material properties (layer like structure, brine pockets etc) create a complicated stress pattern in the ice. The layered structure that was observed probably created weak zones from which cracks could initiate. But it is not clear how and when the horizontal cracks were formed, and if they were shear or tensile driven. Several investigators have examined the formation of tensile driven cracks in an ice sheet. Shkhinek et al. (1997) has used theory of waves in elastic media and Coloumb-Mohr criterion with reduced tensile stress fracture limit. Their simulations predict long tensile driven cracks for low rates of penetration. Experiments performed by Sodhi (1991) seem to confirm these results. Schulson and Nicolayev (1997) have done compression experiments in the laboratory, and found that horizontal splitting did occur for high confinement. These simulations and experiments were not performed to investigate creep buckling, so they can not be used as a proof of our observations. But they do support the point that horizontal splitting may be involved in a ridging process, and that these cracks may be tensile driven.

7. CONCLUSIONS

The formation of a ridge-field in the Tempel fjord on Spitsbergen was observed and monitored. The ridge-field was about 3 km long, and sail heights up to 1 m and keel depths up to 6 m were typical. The keels were basically situated between the visible sails. The movement of the Tuna glacier probably provoked the ridging, and its speed was measured to 0.23 m/day.

The measured porosity of the ridge-field ranged from 6 % in early March to around 30 % in mid May. The increase in porosity is due to formation of new ridges during the spring. The salinity varied from 4 ppt in old parts to 29 ppt in a younger part of the ridge field. These measurements indicate that substantial brine drainage occurred.

The level ice deformed in creep buckling before fracturing and ridging. The basic failure mode was bending, but horizontal splitting or shearing seems to have been involved in the ridging process.

Acknowledgement

We would like to thank the siv.ings Guro Kjestveit, Arne Langeland and Jon Endre Flåtten and the master student Martin Dahl Grønnevet for their very important assistance during the fieldwork.

8. REFERENCES

Hopkins, M.A. and Tuhkuri, J. 1998. Simulation of ridging and rafting in first-year sea ice.

In: Proceedings of the 14th International Symposium on Ice (IAHR), Potsdam, New York, July 27-31, 1998, Vol. 1, pp. 623-630.

Kjestveit, G. 1998. Mapping of ice ridges in the Tempel fjord and in the Van Mijen fjord on Svalbard the winter of 1998. The University Studies on Svalbard (UNIS) / the Norwegian University of Technology and Science (NTNU), 33 p.

Leppäranta, M., Lensu, M., Kosloff, P. and Veitch, B. 1995. The life story of a first-year sea ice ridge. Cold Regions Science and Technology, Vol. 23, pp. 279-290.

Løset, S., Langeland, A., Bergheim, B. and Høyland, K.V. 1998: Geometry and Physical Properties of a Stamucha found on Spitsbergen. In: Proceedings of the 14th International Symposium on Ice (IAHR), Potsdam, New York, July 27-31, 1998, Vol. 1, pp. 339-344.

Parmerter, R.R. and Coon, M.D. 1973. On the mechanics of pressure ridge formation in sea ice. Offshore Technology Conference, paper number OTC 1810. 6200 North central Expressway, Dallas, Texas 75206, USA.

Parmerter, R.R. and Coon, M.D. 1972. Model of pressure ridge formation in sea ice. Journal of geophysical research. Vol. 77, No 33, pp. 6565-6575.

Tuhkuri, J., Lensu, M., and Hopkins, M.A. 1998. Laboratory and field studies on ridging of an ice sheet. In: Proceedings of the 14th International Symposium on Ice (IAHR), Potsdam, New York, July 27-31, 1998, Vol. 1, pp. 397-404.

Sanderson, T.J.O. 1988. Ice Mechanics, risk to offshore structures. Graham and Trotman, London, 253 p.

Schulson, E.M. and Nickolayev, O.Y. 1995. Failure of columnar saline ice under biaxial compression: Failure envelopes and the brittle-to-ductile transition. Journal of geophysical research, Vol. 100, No B11, pp. 22383-22400.

Shkhinek, K., Kapustiansky, S., Jilenko, A., Blanchet, D. and Kärnä, T. 1997. Ice, velocity, load. Proceedings of RAO'97 conference (in print)

Sjølind, S.G. 1984. Viscoelastic buckling of beams and plates on elastic foundation. In: Proceedings of the 7th International Symposium on Ice (IAHR), Hamburg, August 27-31, 1984, Vol. 1, pp. 63-72.

Sodhi, D. 1991. Ice-structure interaction during indentation Tests. In: Proceedings of the Ice-Structure Interaction IUTAM-IAHR Symposium, pp. 619-640.

Tverberg, V. (ed.) 1994. Data rapport feltkurs 7. – 15. april 1994. Internal report from field course in AGF-202, Arctic Oceanography, The University Studies on Svalbard (in Norwegian), 70 p.

Chapter 7

Scaling and measurements of ice rubble properties in laboratory tests

Proceedings of the 15th International Symposium on Ice (IAHR), Gdańsk, Poland, 28 August – 1 September 2000, Vol. 1, pp. 105-112.

Notation

Symbols:

d	diameter
r	radius
h	height / thickness
λ	scaling unit
c	cohesion
φ	angle of internal friction
T	temperature
m	mass
F	average material resistance / force
g	acceleration due to gravity
α	angle between shear plane and vertical plane
σ	normal stress
τ	shear stress
H	hardness
S	surface

Indices:

f	freezing point
sn	snow
ba	steel ball
b	buoyancy
k	keel
eff	effective keel
α	angle between shear plane and vertical plane
bs	steel ball - snow

Scaling and measurement of ice rubble properties in laboratory tests

Arnor Jensen[1,3], Knut V. Høyland[1] and Karl-Ulrich Evers[2]
[1]The Norwegian University of Science and Technology (NTNU), Norway
[2]Hamburgische Schiffbau-Versuchsanstalt (HSVA), Germany
[3]Barlindhaug Consult as, Norway

ABSTRACT

Physical and mechanical properties of level ice and ice ridges have been scaled and determined in laboratory tests. Tempering the ice surface scales the strength of the level ice, the unconsolidated ice rubble is as in nature already at the freezing point and this makes a temperature scaling impossible. Small-scale mechanical tests showed that the ice blocks from the ridge were stronger than the level ice. Salinity and ice temperature profiles were measured. Ice rubble properties in three trapezoidally shaped ridges were investigated. The consolidated layer was cut along the perimeter of a circular plate (d=0.7m), and the plate was loaded vertically in order to penetrate through the ice ridge. The force and displacement of the plate were recorded simultaneously. Results from the tests are reported together with material properties derived from a simplified analytical model.

INTRODUCTION

Sea ice ridges are formed by compression or shear in the ice cover. They consist of an overwater part (the sail) which is a mixture of ice blocks, air and snow, and an underwater part (the keel) in which there are ice blocks and water. The keel is divided into a consolidated - and an unconsolidated part. First-year sea ice ridges are major obstacles to transport and operations in waters where first-year ice prevails, such as the Pechora Sea, the Barents Sea and the Baltic Sea. The load these ridges may exert on a ship or a structure is not well known and the present load algorithms seem to overestimate the real loads (Timco et al., 1999). Laboratory work is a vital part of the strive to gain insight into the ridge-structure interaction process and, thereby improve the load estimates. One of the major problems with laboratory testing is scaling. Scaling is done according to which effects that dominate the problem, gravity, inertia, velocity etc. Gravity forces dominate our problem thus Froude scaling is used. The basic idea here is that the gravity field is not scaled and that the basic scaling unit is the length (λ). Some work has been done on ridge-structure interaction in the laboratory (Keinonen and Nyman, 1989; Eranti et al., 1992; Løset et al., 1998 and Kamesaki and Yamauchi, 1999). However, no standardised method for ridge production in ice facilities seems to exist. The ridges are usually made by cutting the ice manually and making a pile. More advanced and realistic ridge formation has been done in the laboratory by Tuhkuri et al. (1998), but they have not made any mechanical testing of their ridges. Laboratory tests of ice rubble have been done by several authors with different equipment, see Ettema and Urroz-Aguirre (1991) and Timco and Cornet (1999) for an overview of results and methods. The rubble is often considered to be almost cohesionless, and small values of the cohesion (c) is often found, but a wide scatter of values for the angle of internal friction (φ) have been reported. A plug, or a push down test where the consolidated layer is pre-cut and the rubble is loaded vertically was originally done in-situ by Leppäranta and Hakala (1992), and has been done in the laboratory by Azarnejad and Brown (1998). One problem is the derivation of material properties from the recorded force and displacement, as the stresses on the failure plane are not known.

EXPERIMENTS, RESULTS AND ANALYSIS

Procedure for production and consolidation of the ridges

The experiments carried out in the Large Ice Tank of the Hamburg Ship Model Basin (HSVA), were designed to simulate the most severe ice conditions in the Pechora Sea. Løset et al. (1997) gives an overview of the ice conditions in the area. The design level ice thickness was 1.2 m and the design keel depth was 18 m in the testing. The maximum block thickness in such a ridge is about 1.1 m (Tucker and Govoni, 1981 and Sayed and Frederking, 1988). The block size distribution in ridge sails has been examined by eg Veitch et al. (1991) and Kaankanpää (1997). They report that the length and the width of the blocks were between 1.5 and 5 times the thickness. However, it is possible that larger blocks exist in the lower part of the keel (Mauri Määttänen, personal communication).

The model ice sheets were produced according to the procedure described by Evers and Jochmann (1993). The characteristic parameter of the level ice was the flexural strength, because the predominant ice failure mode in ice-ship interaction is bending. The proper flexural strength was obtained by heating the ice so that the target strength and thickness was reached. The scaling factor λ was equal to 25. The other parameters were scaled according to Froude scaling (see e.g. Løset et al., 1998).

The ridge production procedure is explained in Jensen et al. (2000). Three different level ice sheets were produced with embedded ridges (3000, 4000 and 5000), and three different ridges were tested: 4000, 5001 and 5002. Fig. 1 shows a longitudinal cross-section of ridge 5002.

After the ridge formation the freezing continued until the target level ice thickness was reached (48 mm). The level ice growth during the consolidation period was about 10 mm. The ridge was examined after each test by cutting it into pieces and inspecting it visually. The thickness of the consolidated layer was between 10 and 15 cm. The results are comparable to what Timco and Goodrich (1988) found in their laboratory work.

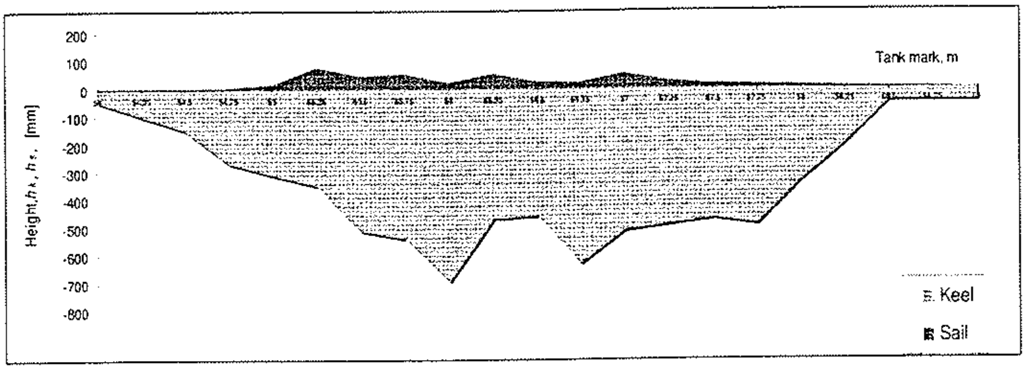

Fig. 1. Longitudinal profile of ridge 5002.

Testing of physical properties; salinity, density and temperature

Measurements were done on salinity, density and temperature development in the level ice and in the ridge. The temperature development in the ridges is shown in Fig. 2. During the consolidation phase the cold front ($T < T_f$) advanced less than 5 cm below the water line, i.e. the internal redistribution of heat was essential to explain the observed consolidation thickness of 10 – 15 cm. The temperature at the ice/water interface was constantly at the freezing point (T_f = -0.5°C). Warming-up of the ice is necessary to obtain the correct scaled flexural strength. The temperature profile shows that the consolidated layer and the keel was colder than the surface of the level ice, i.e. at the freezing point or below.

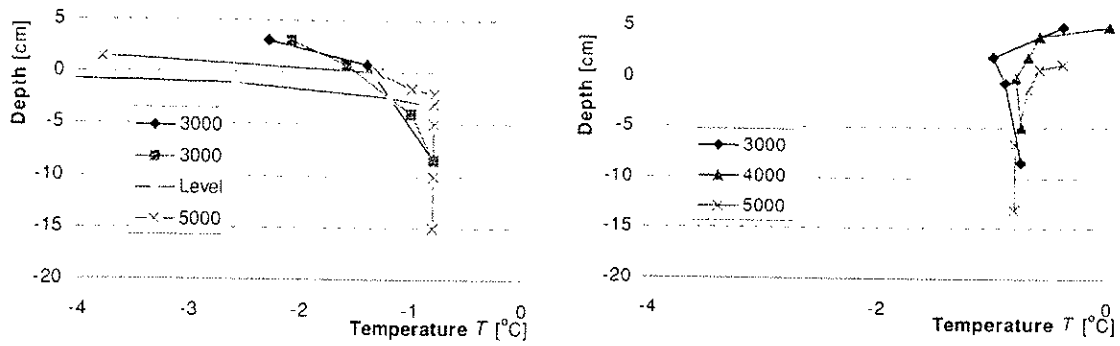

(a) (b)

Fig. 2. Temperature profiles a) during consolidation process and b) prior to testing.

Table 2 displays the salinity and density measurements. 38 samples of the level ice and the ridges were taken for salinity measurements. Little difference was found between the level ice (3.46 ppt) and the keel (3.35 ppt), but the salinity in the sail (3.18 ppt) was a bit lower. It was a clear trend of decreasing salinity with time; it decreased about 0.8 ppt per day. The salinity of the water in the basin was 8.5 ppt. Ten measurements of density were done (8 by the mass divided by volume method, 1 with mass and buoyancy and 1 with volume and buoyancy.

Table 1. Salinity and density.

	Density (kg/m^3)	Salinity (ppt)		
		Sail	Keel	Level ice
Average value	867	3.18	3.35	3.46
Standard deviation	49	0.84	0.64	0.36
Number of samples	10	14	5	18

Testing of mechanical properties of the level ice and individual ridge blocks

Two tests were carried out to examine the mechanical properties: beam bending and a hardness test. In the hardness test two different steel balls were used. They were dropped from a certain height h_{ba} (20 or 25 cm) and the indentation diameter, d_{sn}, and the penetration depth, h_{sn}, were measured by a slide gauge. The mass of the steel balls, m_{ba}, were 90 and 150 g, and the diameter, d_{ba}, 28.3 and 33 mm respectively. This kind of testing is described by Moldestad (1999). The energy balance in Eq. 1 defines an average material resistance $\overline{F_{sn}}$:

$$m_{ba} \cdot g(h_{ba} + h_{sn}) = \int_0^{h_{sn}} F_{sn} dh = \overline{F_{sn}} \cdot h_{sn} \qquad (1)$$

where h_{sn} is the penetration depth.

The hardness, H, is defined as the material resistance divided by the contact area between the ice and the steel ball (S_{bs}):

$$H = \frac{\overline{F_{sn}}}{S_{bs}} \tag{2}$$

The test results showed a significant scatter, however a general trend was seen and average values are summarised in Table 2. The strength decreased with increasing temperature.

Table 2. Mechanical properties from sheet 5000 (number of drop tests in brackets).

Testing time (h)	15:00	16:00	20:00	22:00
Approx. bending strength, σ_b (kPa)	55-60	45-55	20-30	15-20
Hardness of level ice, H (kPa)	65 (18)	58 (3)	13 (2)	22 (2)
Hardness of cons. layer, H (kPa)			94 (6)	252 (8)
Hardness of sail, H (kPa)			69 (2)	
Hardness of refrozen pocket, H (T-ice) (kPa)			76 (2)	

Ridge penetration test

The sail was removed and the consolidated layer was cut. Fig. 4 shows the set-up. The circular ballasted plate was hanging in a crane and lowered carefully down so that it smoothly touched the ice. Zero of the load cell was taken and the plate was lowered further down until it was obvious that the ridge had failed. After failure, the plate was lifted up, re-lowered and finally lifted up again. The velocity of the crane was constant and force and displacement versus time were recorded. Fig. 3 shows a typical force and displacement curve versus time for the testing and Table 4 shows the key values calculated from the tests. The angle α is found by adjusting the calculated buoyancy force to the measured one.

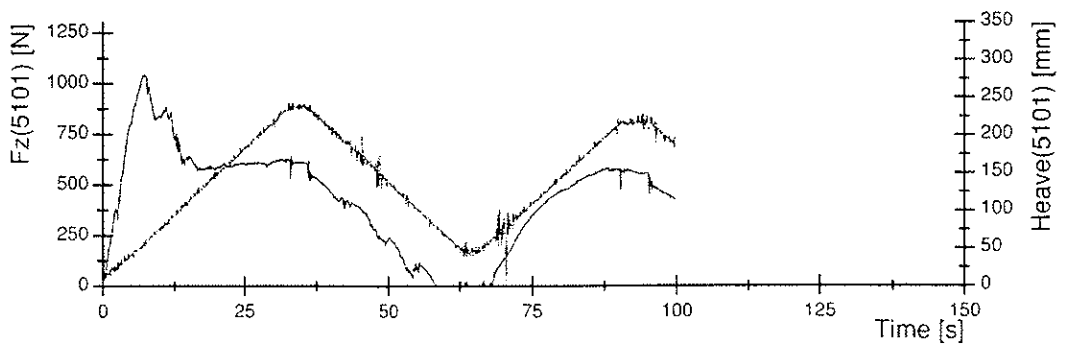

Fig. 3 Force and displacement curve during testing.

Table 3. Key values from the measurements

Test	F_{max}	F_b (max load)	F_b (max displ.)	h_k	h_{eff}	Radius	α
4000	1274 N	324 N	677 N	0.550 m	0.450 m	0.35 m	33.5°
5001	1043 N	259 N	612 N	0.559 m	0.499 m	0.35 m	22°
5002	818 N	276 N	629 N	0.559 m	0.499 m	0.35 m	25°
5003	758 N	97 N	124 N	0.559 m	0.499 m	0.10 m	31°

A simple analytical analysis of the plug test is done as follows. A failure plane with stresses τ_α and σ_α as shown in Fig. 4a) is assumed. The vertical distribution of stresses is assumed to be linear as shown in Fig. 4b), where $\tau_\alpha = 2 \cdot \overline{\tau}$ and $\sigma_\alpha = 2 \cdot \overline{\sigma}$.

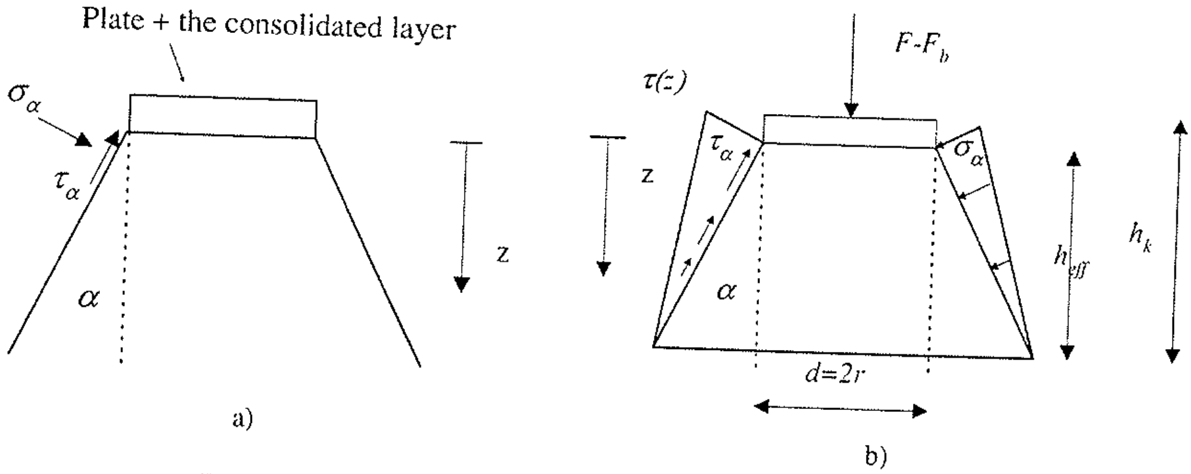

Fig. 4. Simple analytic model for shear punch analyses.

Vertical equilibrium of the cone in Fig. 4 b) and the Colomb-Mohr yield criterion give the following two equations:

$$\overline{\tau} = \frac{F - F_b}{\cos\alpha \cdot S} + \overline{\sigma} \cdot \tan\alpha \quad (3)$$

$$\tau_\alpha = c + \sigma_\alpha \cdot \tan\varphi \quad (4)$$

where F is the applied force, F_b the buoyancy force and S the surface on which the stresses act, c is the cohesion and φ the angle of internal friction.

This gives us two equations and four unknowns. When the normal stress on the failure plane is between the limits given in (5), the extreme values for the material parameters presented in Table 5 can be calculated.

$$\frac{F}{3 \cdot \pi \cdot r^2} < \sigma_\alpha < \frac{F}{\pi \cdot r^2} \qquad (5)$$

where r is the radius of the plate.

Table 4. Extreme values for c and φ if σ_α is between the limits given in Eq. 5.

	Test #		
	4000	5001	5002
c_{max} (Pa)	3338 – 1915	2423 – 1622	1895 – 1174
φ_{max} (-)	45 – 61	42 - 61	44 – 61

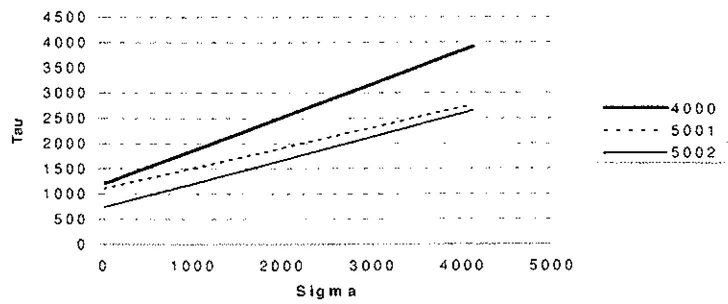

Fig. 5. The equilibrium equation for the three plug tests

In Fig. 5 the equilibrium equations for the three tests are shown. If we assume that the same material properties yield for the two ridges and that the normal stress on the failure plane is the bigger in test 4000 and the smaller in the 5002 test, then the following range of the material parameters c and φ can be estimated: c < 500 Pa and 25° < φ < 40°

DISCUSSION AND CONCLUSIONS

The ratio of the thickness of the consolidated layer to the thickness of the model level ice was 2 – 3, this is higher than what has been found in the real world (see eg Frederking and Wright, 1982; Kaankanpää, 1997 and Leppäranta and Hakala 1992). 3 – 4 layers of refrozen rafted ice were also observed in the unconsolidated part of the keel, this may be more than what exists in a real ridge.

The hardness, H, found from the drop test is not a well-defined material parameter in relation to the flexural strength, thus it can only be used as an index value. Measurements of the flexural strength and the hardness show that the ice in the ridge was too strong compared to the level ice. It is well known that the ice strength decreases with increasing temperature. and the temperature difference between the level ice and the ridge keel explains the difference in strength. In nature the temperatures in the unconsolidated rubble are at the freezing point, whereas the average temperature of the level ice is normally below T_f.

The analytical solution does not give exact material properties as the stresses on the failure plane are unknown, but we suggest $c < 500$ Pa and $25° < \varphi < 40°$. The cohesion has the dimension Pa and should thus be scaled with a factor 25, this gives a full-scale cohesion of $c < 12$ kPa. The material properties of unconsolidated ice rubble are not yet well established, but our suggested values are comparable to what others have found (Ettema and Urroz-Aguirre, 1991).

Acknowledgement

The authors would like to thank the Hamburg Ship Model Basin (HSVA), especially the ice tank crew, for the hospitality, technical support and professional execution of the test programme in the ARCTECLAB. The research activities carried out at the Large Scale Facility ARCTECLAB were granted by the TMR Programme from the European Commission through contract N°ERBFMGECT950081. We would also like to thank the initiator of the project professor Sveinung Løset for practical support and interesting discussions, Denis Tazov for helping us during testing and for being a magician with computer graphics and apples. Navion and Statoil provided additional financial support without which the tests would not have become what they did.

References

Azarnejad, A. and Brown, T.G. 1998. Observations of ice rubble behaviour in punch tests. Proceedings of the 14th International Symposium on Ice (IAHR), Potsdam, New York, USA, July 27-31 1998, Vol. 1, pp. 589-596.

Eranti, E., Lehmus, E. and Nortala-Hoikkanen, A. 1992. First-year ice ridge characteristics and loads on offshore structures. San Francisco, USA, 14-19 June, 1992, pp. 681-687.

Ettema, R. and Urroz-Aguirre, G.E. 1991. Friction and cohesion in ice rubble revisited. Proc. Cold Regions Engineering, West Lebanon, New Hampshire, USA, pp. 316-325.

Evers, K.-U. and Jochmann, P. 1993 An Advanced Technique to Improve the Mechanical Properties of Model Ice Developed at the HSVA Ice Tank , Proceedings of the 12th International Conference on Port and Ocean Engineering under Arctic Conditions (POAC), 17- 20 Aug. 1993, Hamburg, Vol. 2, pp. 877-888.

Jensen, A., Løset, S., Høyland, K.V., Hellmann, J. and Vodahl, B.P. 2000. Model test of an arctic tanker concept for loading oil: Part 2: Barge in a moored loading position. Proceedings of the 15th International Symposium on Ice (IAHR), Gdańsk, Poland, 28 August – 1 September 2000, Vol. 1, pp. 353-362.

Kankaanpää, P. 1997. Distribution, morphology and structure of sea ice pressure ridges in the Baltic Sea. Fennia 175:2, pp. 139-240. Helsinki. ISSN 0015-0010.

Kamesaki, K. and Yamauchi, Y. 1999. Experimental study for first-year ridge load. Proceedings of the 9th international offshore and polar engineering conference (ISOPE), Brest, France, 30 May-4 June 1999, Vol. 2, pp. 518-522.

Keinonen, A. and Nyman, T. 1978. An experimental model scale study on the compressible, frictional and cohesive behaviour of broken ice mass. Proceedings of the 10th international conference on ice (IAHR), Luleå, Sweden, 12-16 June 1989, Vol. 2, pp. 335-353.

Leppäranta, M. and Hakala, R. 1992. The structure and strength of first-year ridges in the Baltic Sea. Cold Regions Science and Technology, 20 (1992), pp. 295-311.

Løset, S., Kanestrøm, Ø. and Pytte, T. 1998. Model tests of a submerged turret loading concept in level ice, broken ice and pressure ridges. Cold Regions Science and Technology 27 (1998), pp. 57-73.

Moldestad, D. A. 1999. Some aspects of ski base sliding friction and ski base structure. Dr Thesis Dep. of Structural Engineering, NTNU, Trondheim, Norway, ISBN 82-7984-019-2, ISSN 0802-3271, 197 pages.

Sayed, M. and Frederking, R.M.W. 1988. Measurements of ridge sails in the Beaufort Sea. Canadian Journal of Civil Engineering 16, 16-21.

Timco, G.W. and Cornet, A.M. 1999. Is φ a constant for broken ice rubble? Proc. 10th workshop on river ice management with a changing climate, J.C.Doering Ed., Winnipeg, Mantioba, Canada, 8-11 June 1999, pp. 318-331.

Timco, G.W., Wright, B., Johnston, M. and Frederking, R. 1999. First-year ice ridge loads on Molikpaq. Proceedings from the 4th International Conference on Development of Russian Arctic Offshore (RAO), St. Petersburg, Russia, 6-9 July 1999, Vol. 2, pp. 172-179.

Timco, G.W. and Goodrich, L.E. 1988. Ice rubble consolidation. Proceedings of the 9th International Symposium on Ice (IAHR), Sapporo, Japan, pp. 426-438.

Tucker III, W.B. and Govoni, J.W. 1981. Morphological investigations of first-year sea ice pressure ridge sails. Cold Regions Science and Technology, 5, 1-12.

Tuhkuri, J., Lensu, M. and Hopkins, M.A. 1998. Laboratory and field studies on ridging of an ice sheet. Proceedings of the 14th International Symposium on Ice (IAHR), Potsdam, New York, USA, July 27-31 1998, Vol. 1, pp. 397-404.

Veitch, B., Lensu, M., Riska, K., Kosloff, P., Keiley. P. and Kujala, P. 1991. Field observations of ridges in the northern Baltic Sea. Proceedings of the 11th International Conference on Port and Ocean Engineering under Arctic Conditions, St. John's, Canada, pp. 381-400.

Chapter 8

Summary, conclusions and recommendations for further work.

8.1 Summary and conclusions

Simulations and measurements have been performed. Four different in-situ ridges and the surrounding level ice conditions as well as three laboratory made ridges have been studied. Geometry, morphology and salinity were examined in the four field ridges, three on Spitsbergen and one in the Gulf of Bothnia. Measurements of spatial and temporal temperature development were done in three ridges, the density and the crystal structure were studied in two ridges, and small-scale uniaxial compression tests of the consolidated layer were only done on ice from one ridge. The formation of a ridge-field and the creep buckling of the level ice prior to ridging were the main objectives of the fourth field-study. Three ice sheets with embedded ridges were produced in the Large Ice Tank of the Hamburg Ship Model Basin (HSVA). Examinations of salinity, density and temperature development, small-scale mechanical testing and a plug test were performed. In the plug test the consolidated layer was cut and the rubble loaded vertically until failure.

A numerical finite element model to study the heat transfer processes in first-year sea ice ridges has been developed. The program ABAQUS with user-defined subroutines to calculate the thermal load has been applied. The four surface heat fluxes: the sensible flux (q_{sens}), the sublimation flux (q_{subl}), the long-wave flux (q_{long}) and the short-wave flux (q_{sol}) constituted the thermal load. They were calculated by the use of the surface temperature of the ridge, the meteorological data and the spatial and temporal location. The porosity of the ridge has been treated in two different ways; 1) creating a composite material consisting of sea ice and water with ordinary sea ice/water thermal properties and 2) defining a homogeneous equivalent material.

The main conclusions are the following:

- The ratio of the thickness of the consolidated layer divided by the thickness of the surrounding level ice, R_{avg} has been estimated based on temperature measurements, drillings and in one case, sampling and small-scale mechanical testing:
    1. Temperatures R_{avg} = 1.39, 1.61 and 1.42
    2. Drillings R_{avg} = 1.68, 1.60 and 1.85
    3. Small-scale mechanical tests R_{avg} = - , - and 1.45

- The results from the mechanical testing corresponded better with the temperatures than with the drillings. The temperatures are minimum values but still the drillings probably included a partly consolidated layer.
- The growth of the consolidated layer ranged from 0.45 to 1.02 cm/day, and did not depend on the method of investigation.
- R_{avg} increased in all the in-situ investigations.
- The consistency of the ridge keel differed considerably; this is explained by the different oceanographical conditions in the Van Mijen fjord and in the Gulf of Bothnia as well as by different ridge keel geometries.
- The measured growth of the consolidated layer and the level ice has been simulated with the numerical model. A model with internal conductive heat transfer simulates the measurements well.
- The theoretically derived relationship between the macro porosity, η and the total porosity, η_t seems to be confirmed by the simulations.
- The porosity of the unconsolidated rubble and the thickness of the snow cover are the most important material parameters.

- The initial phase of consolidation seems to be dominated by internal convection, and modifications of the model have to be done to handle this phase. An oceanic flux of 0.5 kW/m^2 had to be added to the keel during the first-week of consolidation to simulate the growth of the consolidated layer from the assumed formation and to the start of the measurements.
- Limit values for R have been found, and they correspond with the analytical formula.
- The initial phase seems to be crucial in order to determine whether the limit values can be considered as maximum.
- The average values of the physical properties of the consolidated layer corresponded with those of the level ice. However, the standard deviations were higher for the consolidated zone. A limited number of samples have been tested, but it is an indication that the consolidated layer is a more inhomogeneous material than the level ice is.
- The movement of the Tuna glacier probably provoked the formation of the ridge-field in the Tempel fjord. The speed of the glacier was measured to 0.23 m/day, and up to four parallel ridges developed during the spring. Ice block thicknesses of 0.2 m were observed in a ridge that was made from one metre thick level ice.
- The initial thickness of the consolidated layer seems to be overestimated in ice tank ridges. This may be the result not problems with scaling of the temperature field and different 'oceanographical' conditions in the basin.
- Small-scale mechanical tests of the laboratory produced ice showed that the strength of pieces of ice from the ridge (also the unconsolidated rubble) was higher than that of the level ice. This was because the level ice was warmer than the ice in the ridge.
- The plug tests gave reasonable results compared to what exists in the literature, but 1) the model to derive material properties from the plug test should be closer examined, 2) the material properties of ice rubble is not well established.
- There seems to be a need for further development of the techniques and the procedures for producing ridges in the ice tanks and for scaling their thermal and mechanical properties.

8.2 Recommendations for further work

The following three important directions of continuing this work should be stressed: 1) To make a mechanical model of the consolidated layer and its interaction with the surrounding level ice, 2) To understand the physical and mechanical processes in the heat transfer and phase transformation between submerged ice and surrounding water in relation to ridging, and 3) Create good ways to produce and scale laboratory ridges.

Concerning a mechanical model of the consolidated layer it is vital to relate observed deformation modes to knowledge about the internal structure of a ridge, and create a numerical model that simulates this. Some points seem to be of interest:

- In what way is the consolidated layer different from level ice?
- How important is the vertical temperature profile through the ice?
- In what way does the confinement from the level ice affect the deformation mode and the load?

The effect of the general oceanographical conditions on the thermal and mechanical erosion of ridge keels during the initial phase and as a seasonal development could be examined. It seems to be important to elucidate how vital the initial phase of consolidation is to the maximum thickness of the consolidated layer. The importance of the deterioration of the keel to the growth of the consolidation zone and the mechanical behaviour of the rubble is neither clear. A work such as this requires practical and theoretical work, but one theoretical/numerical aspect seems to be of particular importance: Develop a thermodynamical model of the heat transfer within the level ice or an ice ridge that considers the convection caused by the moving sea water (brine). This could be done by a) Modify of the existing model by adjusting the thermal parameters, and b) Create a new model that allows particles to move around.

The third aspect concerns research in the ice tank, and is of course linked to the two former aspects. But laboratory experiments brings in the problem of scaling, and this is a fundamental problem in ice mechanics. Two important aspects are the effect of the initial ice temperature profile and the effect of currents and turbulence in the underlying water.